San Jose State University
SJSU ScholarWorks

Master's Theses | Master's Theses and Graduate Research

1991

A study of stress relaxation in thin aluminum alloy films

Wen-Chi Thomas
San Jose State University

Follow this and additional works at: https://scholarworks.sjsu.edu/etd_theses

Recommended Citation

Thomas, Wen-Chi, "A study of stress relaxation in thin aluminum alloy films" (1991). *Master's Theses*. 172.
DOI: https://doi.org/10.31979/etd.85re-c8hw
https://scholarworks.sjsu.edu/etd_theses/172

This Thesis is brought to you for free and open access by the Master's Theses and Graduate Research at SJSU ScholarWorks. It has been accepted for inclusion in Master's Theses by an authorized administrator of SJSU ScholarWorks. For more information, please contact scholarworks@sjsu.edu.

INFORMATION TO USERS

This manuscript has been reproduced from the microfilm master. UMI films the text directly from the original or copy submitted. Thus, some thesis and dissertation copies are in typewriter face, while others may be from any type of computer printer.

The quality of this reproduction is dependent upon the quality of the copy submitted. Broken or indistinct print, colored or poor quality illustrations and photographs, print bleedthrough, substandard margins, and improper alignment can adversely affect reproduction.

In the unlikely event that the author did not send UMI a complete manuscript and there are missing pages, these will be noted. Also, if unauthorized copyright material had to be removed, a note will indicate the deletion.

Oversize materials (e.g., maps, drawings, charts) are reproduced by sectioning the original, beginning at the upper left-hand corner and continuing from left to right in equal sections with small overlaps. Each original is also photographed in one exposure and is included in reduced form at the back of the book.

Photographs included in the original manuscript have been reproduced xerographically in this copy. Higher quality 6" x 9" black and white photographic prints are available for any photographs or illustrations appearing in this copy for an additional charge. Contact UMI directly to order.

U·M·I

University Microfilms International
A Bell & Howell Information Company
300 North Zeeb Road, Ann Arbor, MI 48106-1346 USA
313/761-4700 800/521-0600

Order Number 1344318

A study of stress relaxation in thin aluminum alloy films

Thomas, Wen-Chi, M.S.

San Jose State University, 1991

U·M·I
300 N. Zeeb Rd.
Ann Arbor, MI 48106

A STUDY OF STRESS RELAXATION IN THIN ALUMINUM ALLOY FILMS

A Thesis

Presented to

The Faculty of the Department of Materials Engineering

San Jose State University

In Partial Fulfillment

of the Requirements for the Degree

Master of Science

By

Wen-Chi Thomas

May, 1991

APPROVED FOR THE DEPARTMENT OF MATERIALS ENGINEERING

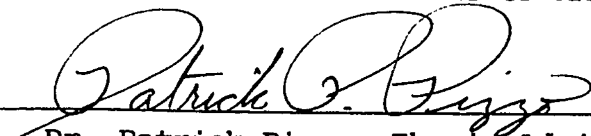

Dr. Patrick Pizzo, Thesis Advisor

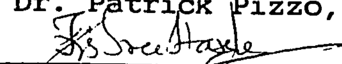

Dr. K. S. Sree Harsha, Department Chairman
of Materials Engineering

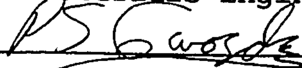

Dr. Peter Gwozdz, Director, Center for
Electronic Materials and Devices

Mr. Burt Masters, Professor of
Materials Engineering

APPROVED FOR THE UNIVERSITY

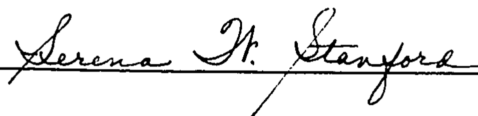

ABSTRACT

A STUDY OF STRESS RELAXATION IN THIN ALUMINUM ALLOY FILMS

by Wen-Chi Thomas

The stress relaxation kinetics of continuous Al thin films on silicon substrates were examined to extract the stress exponent and activation energy associated with time dependent flow at intermediate temperatures (0.45 T_m). For Al-0.5%Cu-1.5%Si films, the activation energy associated with stress relaxation was found to be 13,600 cal/mole, essentially identical to the value for grain boundary diffusion. The stress exponent was found to be large (approximately n = 9) indicating that deformation during relaxation maybe highly nonuniform. The results suggest that failure in finely patterned Al interconnects will become more pronounced as the line width is decreased below the average grain size of the alloy. It is proposed that as the line width decreases, the grains in the line become less able to undergo collective accommodation during stress relaxation, and stress induced voiding will result.

ACKNOWLEDGMENTS

The author wishes to extend her gratitude to academic and industrial advisors, Dr. Patrick P. Pizzo (San Jose State University) and Drs. Michael E. Thomas and Irfan Saadat (National Semiconductor Corporation) for their advice and leadership during the entire investigation.

The author would also like to thank the members of my reading committee, Professors K. S. Shree Harsha, Peter S. Gwozdz, Burt Masters and Linda L. Clements for their helpful technical comments and critique of this study.

Most of all, the author would like to thank her parents Dr. Ying-Huan Chow & Mrs. Tseng Liu Chow for their love, support and encouragement. Without them this study would have never occurred.

The author would also like to acknowledge the kind support of Dr. Ilan Blech and Mr. Dov Hirsch of Flexus for modifying the software of the stress gauge used in this study to make the data collection and analysis more straightforward.

Additionally, the author would like to thank National Semiconductor Corporation (Fairchild Research Center) and their technical staff (especially Mrs. Salve Bautista) for their support in the fabrication of the thin films used in this study.

Finally, the author would like to thank Dr. Court Skinner, the Director of Research, for his generous support of this study.

Table of Contents

	Page
SIGNATURE PAGE	ii
ABSTRACT	iii
ACKNOWLEDGMENTS	iv
LIST OF FIGURES	vii
LIST OF TABLES	ix
1. INTRODUCTION	1
2. BACKGROUND	9
3. PRINCIPLES	17
3.1 Nabarro-Herring Creep	17
3.2 Coble Creep	20
3.3 Dislocation Creep	22
3.4 Grain Boundary Sliding	23
3.5 Logarithmic Creep	23
3.6 Mechanical Properties of Al Alloys vs. Temperature	25
3.7 Elastic Modulus of Al and Its Alloys	26
3.8 Stress-Temperature Behavior of Al on SiO_2/Si	29
3.9 Thin Film Stress Relaxation	32
3.10 Metallization Line Failure	36
3.11 Physical Significance of "n", the Stress exponent	37
3.12 Deformation Maps of Ashby	38
4. EXPERIMENTAL	40

Page

5. RESULTS AND DISCUSSION

5.1 General Overview of the Results and Discussion 46

5.2 Stress vs. Temperature Hysteresis for Al Alloys 46

5.3 Linear Thermal Deformation Region for Al Alloy Thin Films 52

5.4 Thermal Hysteresis of SiO_2/(100)Si and SiN_x/(100)Si 52

5.5 Hysteresis of SiN_x/Al/SiO_2/(100)Si - The Transfer Function 59

5.6 Experimental Stress Relaxation Studies 65

5.7 Evaluation of the Stress Exponent from Experimental Stress Relaxation Data 65

5.8 Self Consistent Evaluation of the Activation Energy 73

5.9 Overall Perspective of the Al Thin Film Relaxation 73

6. CONCLUSIONS 81

REFERENCES 83

List of Figures

Figure		Page
1.	Stress distribution in a plasma enhanced chemical vapor deposition (PECVD) SiN_x film deposited over an Al line	2
2.	Research path for mechanical reliability studies of Al alloys	5
3.	A graphic representation of slit-like and wedge shaped voids	14
4.	Nabarro-Herring creep	19
5.	Coble creep	21
6.	Grain boundary sliding plus accommodation	24
7.	Plot of the tensile strength, yield strength and elongation vs. temperature for a 2014 Al alloy	27
8.	Plot of the elastic modulus vs. temperature for polycrystalline aluminum	28
9.	Stress-temperature behavior of Al-2% Cu on SiO_2/Si	30
10.	Characteristic stress relaxation curve	33
11.	Plots to determine stress exponent and the activation energy from the stress relaxation experiments	35
12.	Deformation mechanism map of Ashby for Al films having 10 micrometer grain size	39
13.	Schematic operational description of the optical scanning stress gauge used in these studies	41
14.	Series of hysteresis loops for an Al alloy showing the effect of preconditioning on stress reproducibility with temperature	43
15.	Experimental organization -- plan for analysis	47
16.	Stress vs. temperature hysteresis loop for an Al alloy deposited at a temperature of 280°C	48

Figure Page

17. Stress vs. temperature hysteresis loop for an Al alloy deposited at a temperature of 25°C 49

18. Stress vs. temperature characteristics for Al alloys 53

19. Cyclical data for the linear stress vs. temperature region shown in Fig. 15 54

20. Stress hysteresis loop for SiN_x cycled between room temperature and 500°C 56

21. Stress hysteresis loop for PECVD SiO_2 deposited at 400°C 57

22. Hysteresis loops of Al and SiN_x coated Al thin films used to obtain the transfer function 60

23. Plot of the master transfer function relating the Al thin film stress in free vs. SiN_x encapsulated thin film structures 63

24. Measured and extracted Al alloy stress relaxation curces for thin films with and without a SiN_x passivation layer 64

25. Stress relaxation data for all non-passivated Al alloys deposited at 280°C 68

26. Method for the evaluation of the stress exponent and activation energy 69

27. The grain boundary and lattice diffusion coefficient of pure aluminum vs. reciprocal temperature 71

28. Ln-Ln plot of the $(d\sigma/dt)/D$ vs. (σ/E_y) for all films used in the stress relaxation studies 72

29. Extraction of the activation energy for grain boundary diffusion from a semilog plot of the Ln $[(d\sigma/dt)/(\sigma/E_y)^n]$ vs. reciprocal temperature 74

List of Tables

Table		Page
1.	Summary of initial test conditions and test duration for stress relaxation tests on Al films deposited at a substrate temperature of 280°C	66
2.	Summary of polynomial expressions used to fit the stress relaxation data for Al films deposited at a substrate temperature of 280°C	67

CHAPTER 1

INTRODUCTION

Open metal lines caused by void formation and subsequent cracking in aluminum interconnections less than 3 micrometers wide is a potentially serious problem in the integrated circuit industry. During the back-end processing of a device, aluminum metal films are deposited, patterned, and etched into a series of conductive traces which carry signals around the device. The metallization layer is then covered with a silicon nitride passivation layer at deposition temperatures on the order of 400°C. This passivation, which helps to block mobile ion diffusion (Na^+) into the device, provides corrosion and mechanical damage protection to the Al and enhances multilevel wiring performance.

However, upon cooling after high temperature processing (400°C), the thermal expansion mismatch of the nitride and aluminum alloy films generates a compressive stress in the SiN_x and a corresponding tensile stress in the encapsulated Al alloy. Figure 1(1) shows the calculated distribution of stress in the passivation dielectric using a finite element analysis of this system. It has been proposed that the primary mechanism for aluminum metallization failure is associated with the locked-in

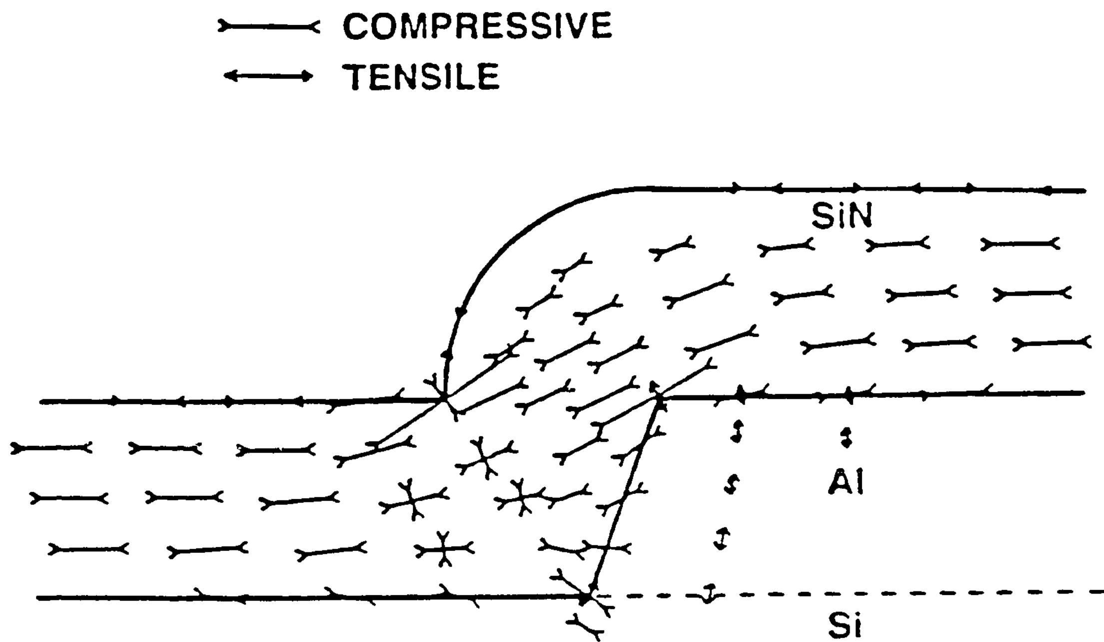

Figure 1. Stress distribution in a plasma enhanced chemical vapor deposition (PECVD) SiN_x film over an Al line. The length and angle of the lines represent the quantity and orientation of stress in the lines.

thermal stress (strain). Localized diffusion of vacancies and motion of dislocations driven by the tensile stress (creep) results in slit-like void formation at grain boundaries[2]. The triaxial tensile stress acting on the passivated aluminum lines is believed to be the key driving force for the enhanced vacancy diffusion and ultimate failure of the lines. These processes proceed until a growing void, acting as a propagating crack, completely spans an Al line and breaks the conductors' electrical path.

Several other variables affecting void induced cracking of interconnects can complicate the kinetics and mode of failure in aluminum lines. These are as follows:

(1) Alloying constituents (i.e., Si, Cu, Ti)
(2) Deposition stresses in the passivation layer
(3) Aluminum grain size (controlled during deposition)
and (4) Aluminum line width

Results to date indicate that stress induced voiding is caused by the application of a sustained triaxial tensile stress on the interconnect. However, it has been shown that the magnitude of room temperature tensile stress decreases during heating to elevated temperature[3]. This stress reduction is caused by a near match to the dimensional state

of the Al and the encapsulating passivation during deposition. In some cases, the stress can change from a tensile to a compressive state[3].

Past studies have attempted to compare different metallizations under accelerated test conditions[4-6] failing to consider the dynamic stress in the analysis of the data. Testing Al under compressive conditions introduces an obvious error in the experimental analysis, for example. Secondly, it is possible during accelerated testing, that the mechanism responsible for failure will not be the same as that observed at lower temperature. It is usually assumed that the mechanism responsible for the stress induced void formation process is the same under all tensile stress test conditions for the entire temperature regime examined.

Figure 2 outlines the proposed research path that will be implemented to characterize the stress induced void formation and failure of fine line interconnects. In the first phase of the study, the stress relaxation characteristics of <u>continuous</u> Al alloy thin films are examined in order to determine the activation energy and stress exponent associated with material flow under tensile stress. In this investigation, thin films of the ternary Al-0.5%Cu-1.5%Si aluminum alloy system are studied.

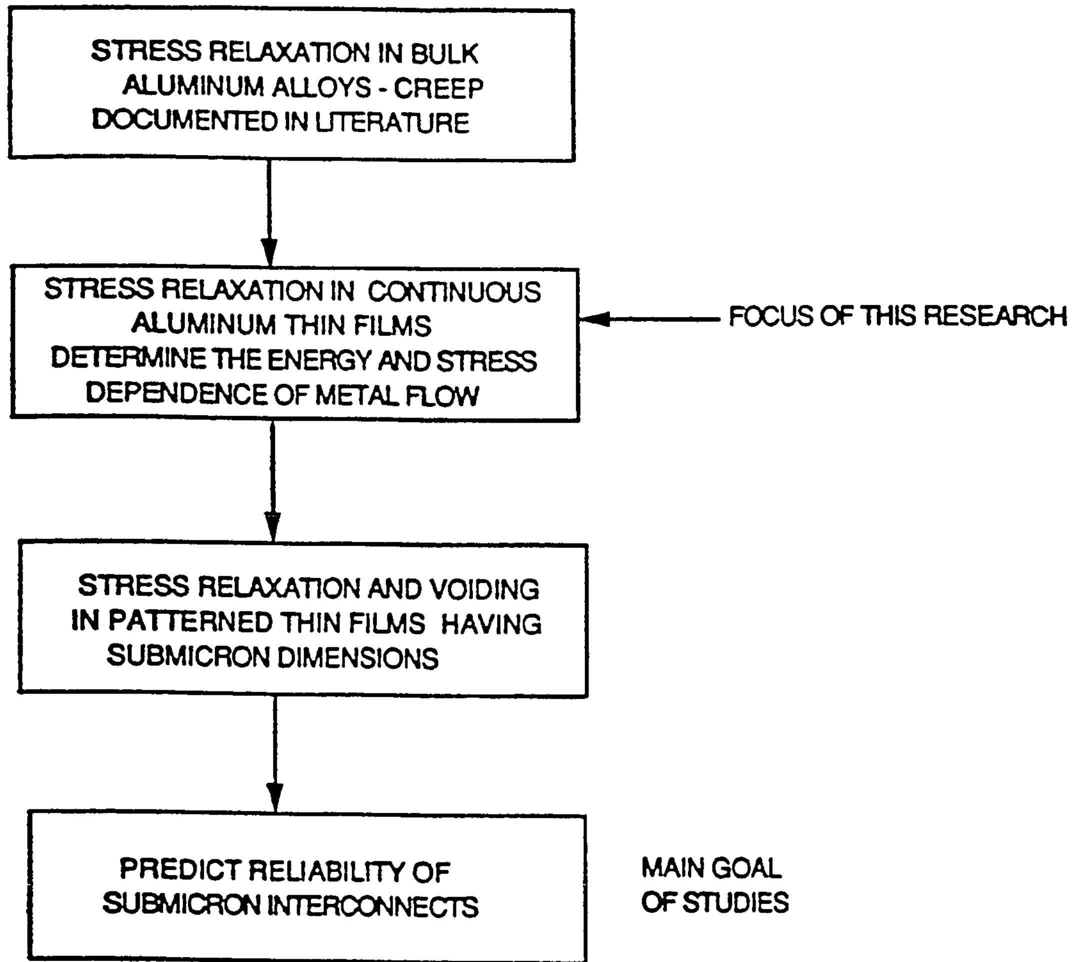

Figure 2. Research path for mechanical reliability studies of Al alloys.

In the second phase of the study, submicron lines of Al will be generated using photolithographic patterning and RIE etching. These lines will be tested for stress relaxation and electrical failure under thermally induced triaxial stress. Electrical and optical monitoring of the line integrity should help ascertain the nature of the failure. The activation energy and stress exponent obtained from the phase I investigation will be compared with values determined from the failure statistics in the phase II work. The data from both phases of the program should allow the development of a better model to describe and predict the reliability of submicron Al lines under large tensile loading.

By using a high temperature stress gauge and knowledge of the thermal hysteresis loop of the Al alloys, it is possible to arrest the heating or cooling cycle at a fixed temperature and tensile stress level. The film stress can then be monitored as a function of time under isothermal conditions to characterize the relaxation process.

Other experiments in the first phase research deal with generating a transfer function to extract the Al alloy film stress from composite films with an overlayer of encapsulating silicon nitride. The Al stress is evaluated at various temperatures and times during hysteresis cycling

and isothermal stress relaxation.

The power law dependence of stress on film strain rate is examined and compared with data extracted from bulk Al alloys. Published literature are used to rationalize the operative diffusion mechanism found. Techniques will be developed to evaluate the activation energy associated with the deformation process and compare the values with those previously reported for bulk materials.

The transient decay behavior during the initial phase of stress relaxation and the resultant stress exponent will be used to infer the degree of nonuniformity of the deformation in the films. Qualitative observations concerning potential failure mechanisms in fine metal lines will be ascertained from these data.

It is felt that the results of these continuous thin film studies, although one step removed from the patterned films (phase II), are needed to establish a sound groundwork for evaluating void formation mechanisms in Al thin films. This knowledge should help identify ways to circumvent stress induced failure. Future studies, which will not be addressed in this report, will be undertaken to directly measure effects of stress and temperature on the failure rate of patterned aluminum lines. Data from the continuous

thin film studies will be used to estimate the stress on interconnects having micron and submicron dimensions. Hopefully, the work performed in this study will provide insight concerning the failure prediction of fine metal wires.

CHAPTER 2

BACKGROUND

Although these studies will focus on stress relaxation in continuous thin films, a review of work related to the failure of discrete interconnect structures will be presented.

There have been numerous publications on stress induced failures of aluminum interconnects by various research groups[(2)(7-15)]. In general, the studies can be categorized in terms of three major areas:

(1) The role of thermally induced differential stresses.

(2) The effect of alloying additions.

(3) The temperature dependence of the thermally activated failure process.

Tensile stress due to the large thermal expansion difference between Al and silicon nitride is unquestionably the dominant factor affecting interconnect reliability. For large flat parallel sheets of metal and dielectric, a stress analysis by Nix[(16)] shows that Al sees little imposed stress from the nitride. However, it is more difficult to describe this stress state when the Al metallization feature

size is on the same scale as that of the thickness of the nitride. This is the case that exists with patterned Al features on VLSI devices having dimensions on the order of one micrometer in size. After passivation deposition and during cooling, the Al alloy experiences a large buildup of hydrostatic tensile stress. The stress analysis of this system is complicated with the distribution of stress still under debate.

In order to account for constraint, a finite element stress model was generated by Groothuis and Schroen(7). This model identified regions of highest stress concentration to be in the upper edge of fine metal lines in the vicinity of oxide steps. For two phase Al-Si alloys, high stress regions were also located in the neighborhood of silicon precipitates. From this work and studies by Yue(8), the largest differential stress should be observed in lines approximately 2 to 3 micrometers in width and in the vicinity of large precipitate particles.

In contrast, Hinode, Owada et al(5) and Hinode et al(9), have suggested that there is a distinct correlation between the linewidth and the failure rate. The wider the line, the less likely failure is to occur. This analysis indicates that the smallest lines are most susceptible to failure.

Review of the literature indicates a number of contradictory studies concerning the role that linewidth plays on stress induced voiding. In general, one would expect that the failure time correlates with:

1) The maximum stress observed in the interconnect and
2) The void rate (cm^3/sec) divided into the cross section of the line times the average width of slit like void.

As more consistent stress testing is performed, this issue should be clarified.

Material complications that must be entertained deal with local stress relaxation during interconnect reduction in cross-sectional area. This effect can complicate the failure statistics. Yost[10] proposed that the termination of area reduction occurs when the available thermal stress is relieved below some threshold value. If stress relief occurs during this process, an error could be introduced into the data analysis.

In light of these considerations, it is important to understand the stress relaxation associated with these thin film Al Alloy metallizations at a moderate fraction of the melting point (about 0.3 to 0.5 T_m). Past high temperature accelerated tests performed on Al metallizations

should be viewed with caution as mechanisms activated at these higher temperatures may differ from those mechanisms which govern stress induced voiding at moderate to low temperatures.

Enhanced failure rates at higher ageing temperatures have been reported by Hinode et al[9], Klema[11], Curry[12] and Herschbein[13]. Papers by Hinode, Kelma and Curry discussed failure of the Al lines caused by the thermal expansion mismatch of Al and SiN_x passivation layers. Kelma's paper also mentioned the formation of a harder, brittle film due to N_2 contamination of the Al during the sputter process. Herschbein's paper discusses on line failure caused by silicon nodule formation. These studies found that failure can take place at the beginning stage of high temperature operating life tests (HTOL). However, it is questionable whether the stress state associated with the failure (probably compressive) was accurately defined and is indicative of the true mode of failure at low temperatures (125°C or less). These studies should be treated as informative but they may not yield an accurate picture of the active service failure unless the stress conditions of the test are defined.

In general, alloy additions which strengthen the Al can reduce the film deformation rate and thus failure. Much

experimental data exists on the effects of alloying constituents on the failure rate of interconnects. Turner and Wendel[14] have stated that stress-induced failure can be reduced in aluminum-1% silicon lines by adding 0.5 to 2.0% copper to the metallization. This addition of Cu strengthens the alloy giving it greater mechanical resistance to deformation under tensile loading. Copper atoms in the lattice or at the grain boundaries can also bind to vacancies in the material. This has an effect of reducing $D_{chemical}$ of the Al-Cu alloy. It is this effect that provides better stress and electromigration resistance[2]. This type of approach was used in studies by Hosoda et al[15], which verified that the simultaneous addition of 0.1wt% copper and 0.15wt% titanium reduced the failure rate in pure aluminum lines. Information from these studies is consistent with work on bulk metals at low temperatures, where alloying constituents were found to reduce vacancy diffusion in grain boundaries and within the grains themselves.

A final area of interest concerned with low temperature failure focuses on the nature of the void formation process itself. Mayumi et al[2] noticed that there are two kinds of voids that form in aluminum metal lines: slit-like and wedge shaped voids (Figure 3).

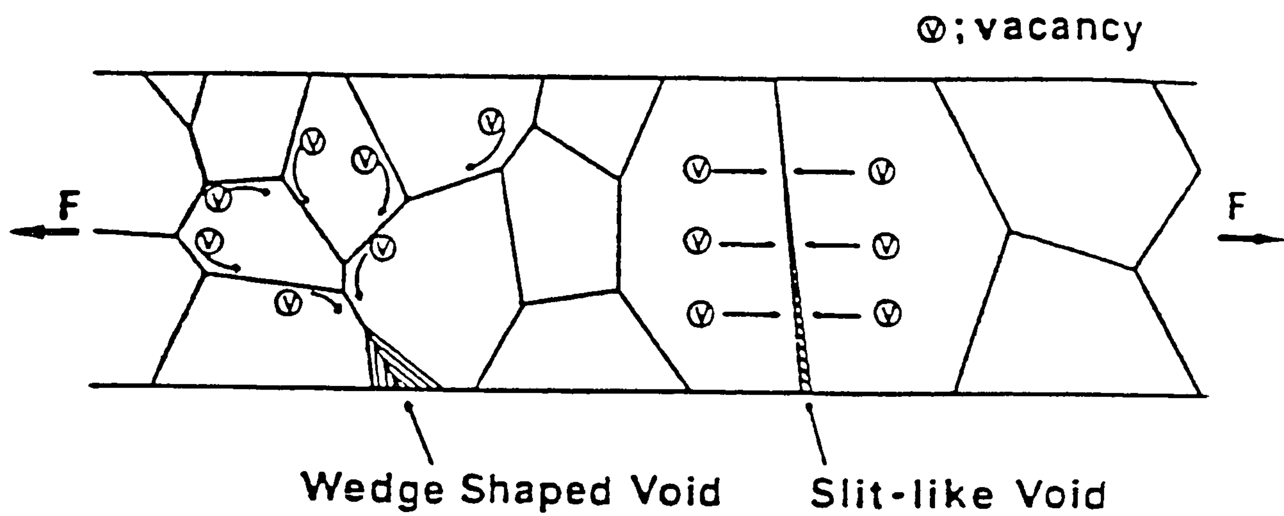

Figure 3. A graphic representation of slit-like and wedge shaped voids.

Slit-like voids cause the lines to have interspersed gaps and are related to possible low angle grain boundaries which are not connected to a grain boundary network. Wedge shaped voids are caused by vacancy diffusion along the grain boundary networks and appear to nucleate at the edges of metal lines. This mode of failure would support a Coble creep or grain-boundary sliding without full accommodation mechanism. These mechanisms will be discussed in the next section of the report.

These past studies have shed great light on the potential mechanisms associated with stress-induced failure. This work will take a step back from fine line failure research and attempt to develop a means to better understand operative stress and deformation in thin film aluminum. This work will hopefully resolve some of the outstanding issues associated with Al deformation and provide a more complete picture of the stress-induced void formation mechanism.

For these studies, it is of interest to determine which of these mechanisms dominates the deformation characteristics of continuous sheet films having a spatial area much larger than the grain size. The grain size of the alloy plays a major role in determining the diffusion mechanism eventually responsible for its failure. This

issue will become important when the grain size and defined metal features are of comparable dimensions as is the case in fine metallization lines which will be studied in phase II of this investigation.

The next section will:

1) Present a more detailed look at the potential stress induced failure mechanisms and
2) Develop the mathematical tools required to extract the activation energy and stress exponent from the Al alloy stress relaxation data.

CHAPTER 3

PRINCIPLES

There are a number of potential failure mechanisms which can contribute to time dependent aluminum deformation and failure: (a) Nabarro-Herring creep, (b) Coble creep (c) dislocation creep and (d) grain boundary sliding. These deformation mechanisms will be described below in greater detail for consideration in the stress relaxation studies.

Before starting this review, it is important to point out that the stress relaxation process actually involves the evaluation of transient creep behavior. Although the failure mechanisms described above are associated with steady state creep, they will be applied to the evaluation of the transient behavior. For the analysis, the steady state creep relationships will be applied to the transient behavior to determine the average activation energy and stress exponent for the active processes.

3.1 Nabarro-Herring Creep

Nabarro-Herring creep is one of the possible atomic transport mechanisms responsible for stress induced failure. The Nabarro-Herring creep mechanism can occur under hydrostatic tension where normal stress components are all

tensile and equal in magnitude. It involves mass transport throughout the grain by a vacancy exchange mechanism. Dislocation motion by glide is assumed to be non-existent for pure Nabarro-Herring transport (Figure 4)(17). However, dislocation climb responsible for subgrain boundary formation, can occur concurrently. It is expected that the Nabarro-Herring mechanism is more likely to dominate when (a) the grain size of the deposited film is much larger than the width of the defined interconnect, (b) the homologous temperature is greater than 0.8, and (c) the thermal driven stress is very low. The expression for Nabarro-Herring creep is as follows(17):

$$\dot{\epsilon}_s = 7\sigma D_v b^3/kTd^2 \qquad [1]$$

where

$\dot{\epsilon}_s$ = steady-state creep rate

σ = applied stress

D_v = lattice diffusivity

b = Burgers' vector

k = Boltzmann's constant

T = absolute temperature

d = grain diameter

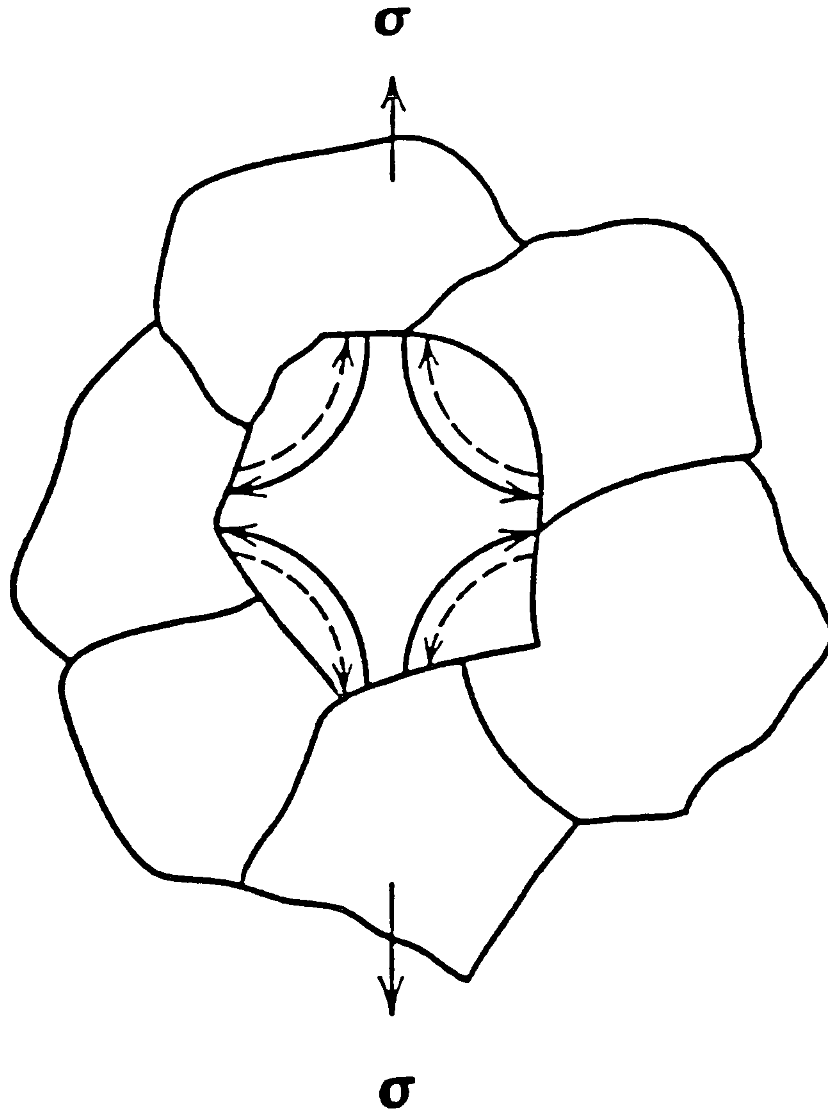

Figure 4. Nabarro-Herring creep (bulk diffusion under a uniaxial tension load). Solid line stands for the direction of vacancy flux and the dashed line represent the direction of atom migration.

3.2 Coble Creep

Coble creep is an alternative atomic transport mechanism which could be responsible for stress induced failure. This creep mechanism also occurs in the range of low stresses and high temperatures. Coble creep is controlled by a grain boundary diffusion process (Figure 5)[18] in which excess vacancies, which are generated in the grain boundaries by stress promote mass transport along the grain boundaries. If the excess vacancies nucleate and grow to form voids in these regions, grain boundary failure can result. This mechanism is expected to be predominant in small grain size films where the interconnect width is much greater than the average grain size. The Coble Creep can be described by the following equation[17]:

$$\dot{\epsilon}_s = 50\sigma D_{gb} b^4 / kTd^3 \qquad [2]$$

where

$\dot{\epsilon}_s$ = steady-state creep rate

σ = applied stress

D_{gb} = grain boundary diffusivity

b = Burgers vector

k = Boltzmann's constant

T = absolute temperature

d = grain diameter

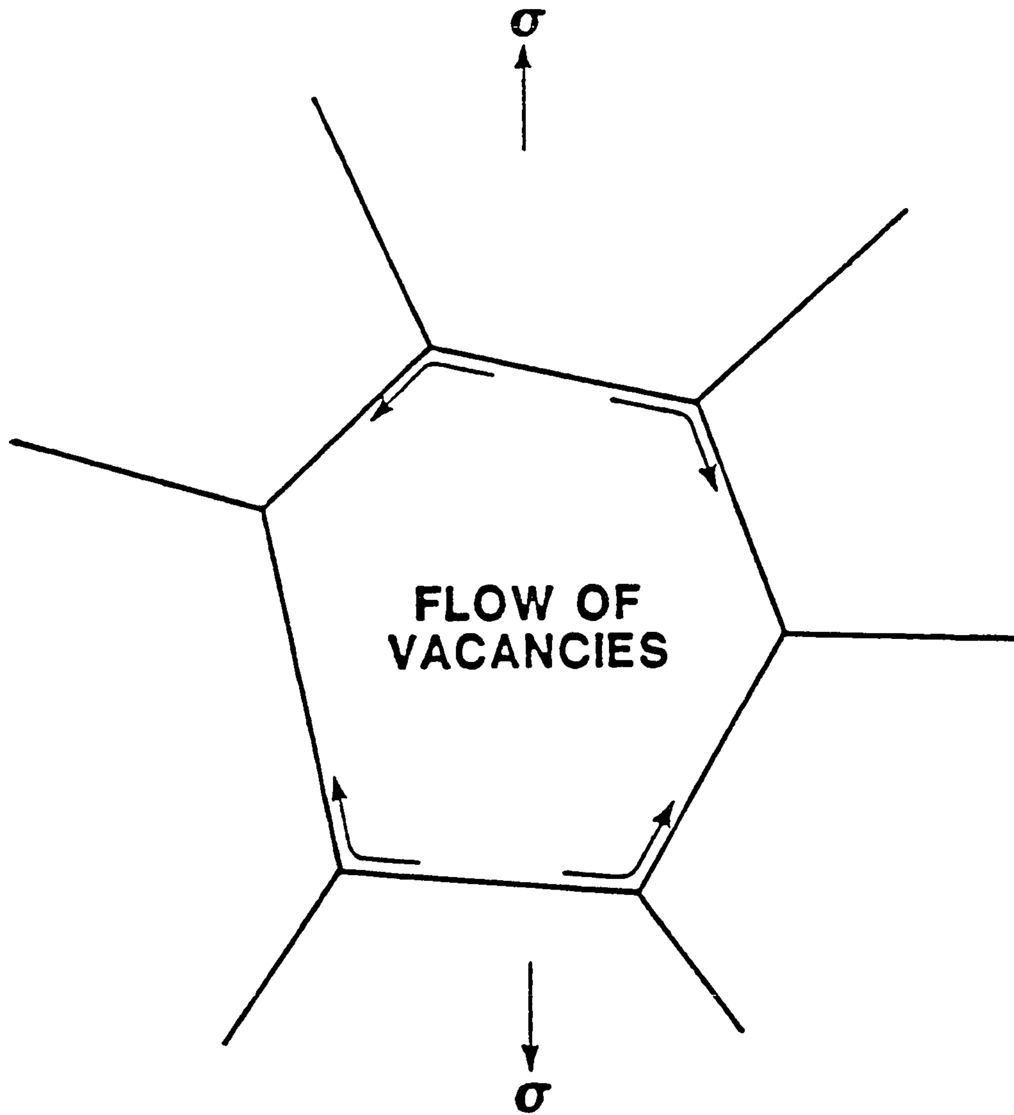

Figure 5. Coble creep (boundary diffusion dominated).

For Coble creep, the deformation process is more critically controlled by grain size than Nabarro-Herring creep.

3.3 Dislocation Creep

Dislocation creep can become an operative mechanism in metal systems having high to intermediate stresses at homologous temperatures greater than one-half. The proposed mechanism is associated with the diffusion controlled movement of vacancies. This mechanism is associated with dislocation climb, where dislocations form subgrain boundaries to reduce the free energy of the body under stress. It has been proposed by Bird(19) that the dislocation creep rate is described by the following relationship:

$$\dot{\epsilon}_s = AD_{gb}/kT\ (\sigma/G)^5 \qquad [3]$$

The terms in the expression have been previously defined for the other failure mechanisms.

Of the mechanisms discussed thus far, dislocation climb has the largest dependence on stress, the typical stress exponent being about 4.5 for polycrystalline metals. As the stress level is increased, a point is reached where the steady-state creep rate no longer follows the above, power-

law relationship. Power-law breakdown occurs; and the stress exponent increases dramatically.

3.4 Grain Boundary Sliding

A fourth potential failure mechanism involves grain boundary sliding (Figure 6)[20]. This process is a separate and distinctively different mechanism from Coble Creep which is grain boundary activated.

At intermediate stress levels and at test temperatures above 0.5 T_m, creep has been shown to be controlled by diffusion induced dislocation movement. However, in this case and under uniaxial loading, the total elongation can have a component contributed by grain boundary sliding. Grains elongate due to stress-induced dislocation climb (Figure 6b); but, the elongation is counterbalanced by grain boundary sliding (Figure 6C). Grain-boundary sliding coupled with stress-induced change in the shape of the grain can be distinguished from the Coble or Nabarro-Herring Creep mechanisms by the stress exponent.

3.5 Logarithmic Creep

A final potential mechanism that will be proposed here deals with logarithmic creep which occurs at low

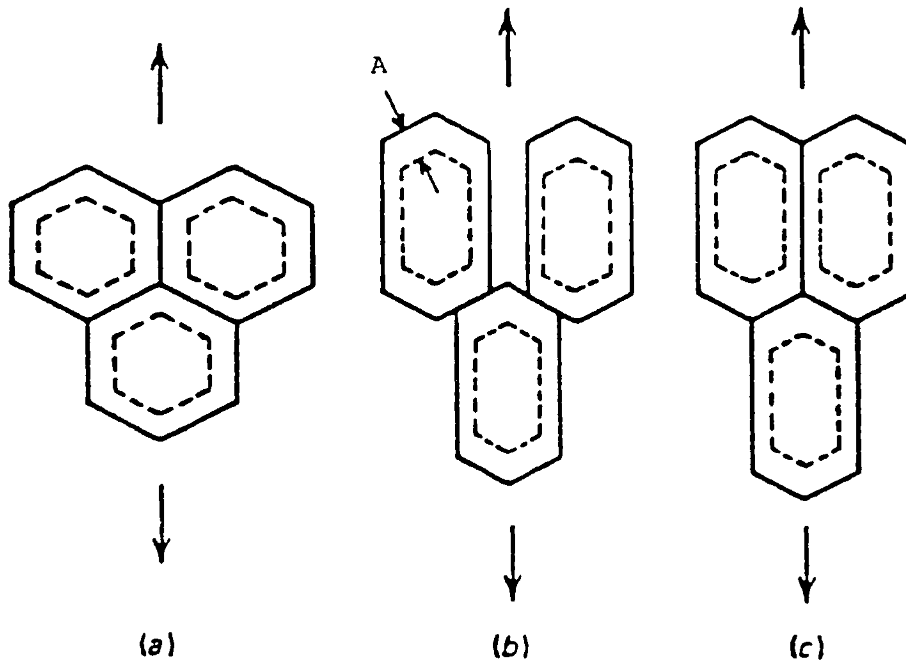

Figure 6. Grain boundary sliding plus accommodation (A is the thickness of a grain boundary).

temperatures and low stress levels. The proposed mechanism involves the flow of dislocations having a range of activation energies. During the initial stressing, dislocations with the lowest activation energy move first causing deformation to occur. Since the temperature is low, recovery and recrystallization are limited and dislocations which first move eventually become pinned by other dislocations or precipitates in the alloy. As these dislocations are "exhausted"(21), the activation energy of remaining dislocation distribution, which is higher, results in a creep rate reduction. Logarithmic creep does not describe the behavior of transient creep adequately.

3.6 Mechanical Properties of Al Alloys vs. Temperature

Before examining the stress relaxation data for the alloys in this study, a brief examination of the properties of bulk Al alloys will be presented. Aluminum alloy (2014) with a composition similar to the material used in this experiment will be examined. It is considered representative of many doped Al alloys. The 2014 alloy has a composition of 4.4%Cu-0.8%Si-0.5%Pb-0.5%Bi with the balance Al and a yield strength comparable to the thin film alloy used in this study. The fine grain size of the thin film alloy will impart greater strength than commercial, bulk alloys at room temperature: but, this is assumed to be

compensated by the higher solute content of the bulk metallization which imparts greater strength to the alloy.

In examining the yield and tensile strengths of the 2014 Al alloy as a function of temperature (Figure 7), it is observed that the strength falls off dramatically between 125°C and 200°C. This behavior is true of most Al alloys and is not very sensitive to the dopant type used for strengthening. Figure 7 also contains a plot of the elongation vs. temperature for this alloy. Up to 150°C, the film does not show a noticeable increase in elongation indicating that grain growth is slow to occur. Above 150°C, grain growth starts to play an important role in reducing yield strength.

3.7 Elastic Modulus of Al and Its Alloys

In evaluating the relaxation properties of polycrystalline Al alloys over a range of temperatures, it is necessary to consider the effect of temperature on the modulus of elasticity. Work performed by McClean and Ishikawa[22], shows a dramatic modulus reduction for polycrystalline Al at intermediate homologous temperatures. Figure 8 shows a plot of the data from their paper. At a temperature of 400°C, a reduction in elastic modulus of approximately 25% from the room temperature value is

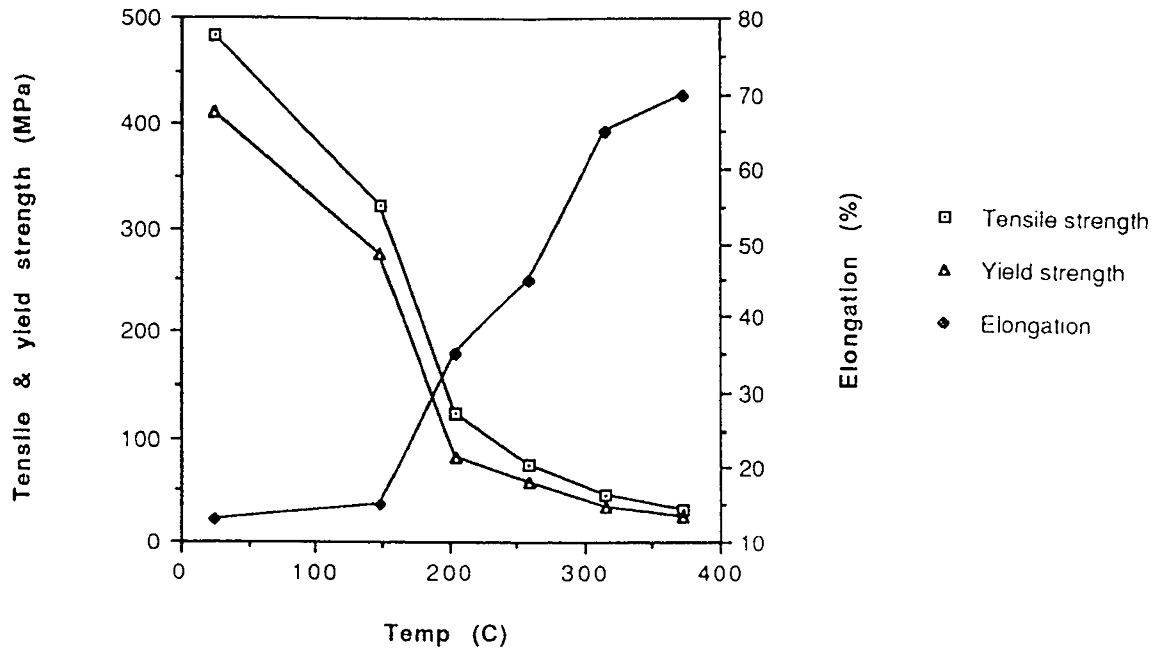

Figure 7. Plot of the tensile strength, yield strength and elongation vs. temperature for a 2014 Al alloy.

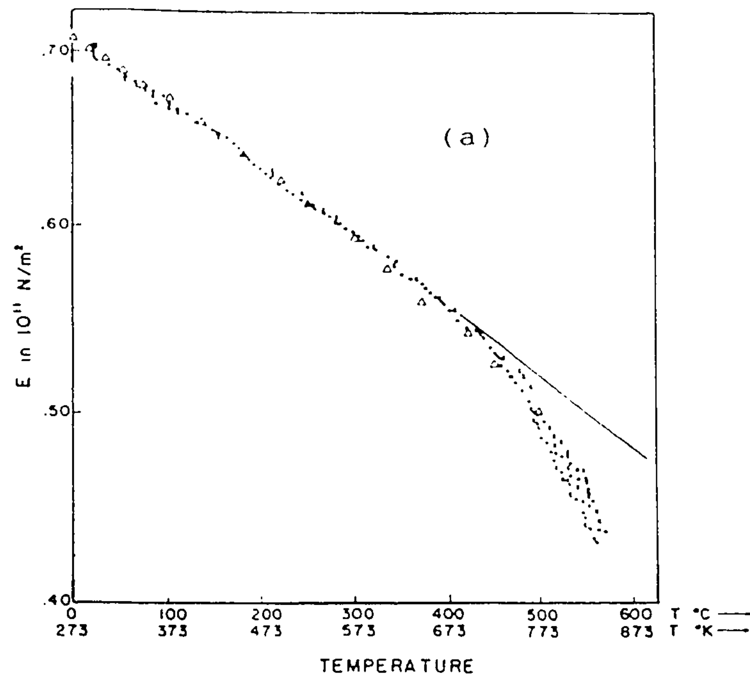

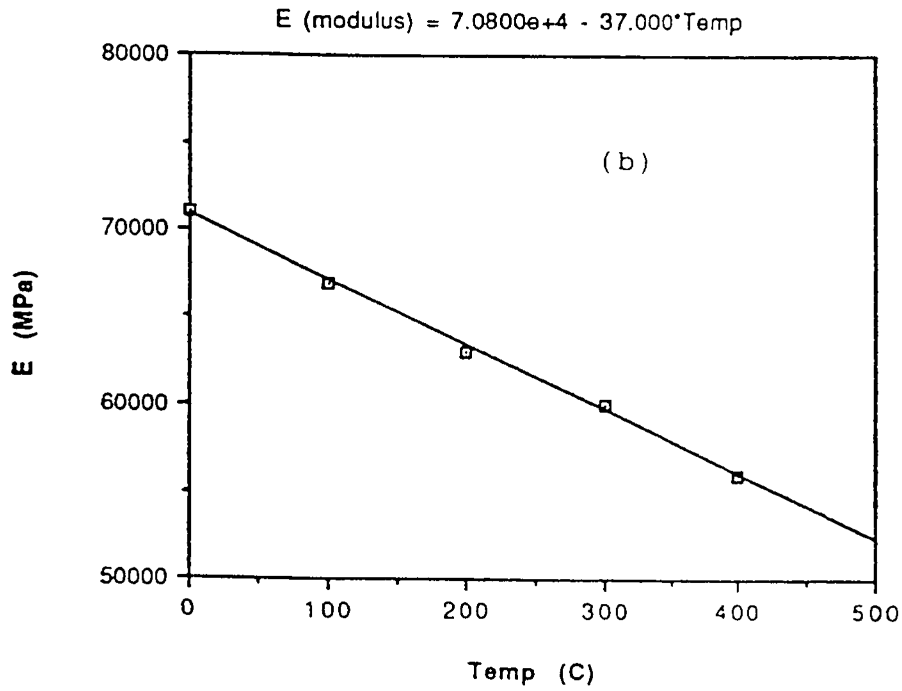

Figure 8. Plot of the elastic modulus vs. temperature for polycrystalline aluminum: (a) Plot from ref. (22) and (b) Linear regression of data in ref. (22)

experienced by the polycrystalline Al films. These data indicate that the modulus of elasticity, which is related to the curvature of the potential between atoms as a function of distance, is strongly dependent on temperature.

The data of McClean, et al, were fit using linear regression [See Figure 8(b)] and the following expression describes the elastic modulus over the temperature range of interest for this study:

$$E_{modulus} = 7.1 \times 10^{4} - 3.7 \times 10^{1}\ T\ (^{\circ}C)\ \text{MPa} \qquad [4]$$

This dependence of modulus on temperature will be used for the stress exponent and activation energy determination.

3.8 Stress-Temperature Behavior of Al on SiO_2/Si

The deformation mechanisms described in the previous sections are driven by differential stresses between the thin Al alloy film and its substrate during thermal cycling. Thin aluminum films on oxidized silicon substrates are subject to a complex stress vs. temperature hysteresis loop during annealing (Figure 9)[3]. The deposition temperature determines where in the loop the film experiences recrystallization, yield, film hardening and grain growth.

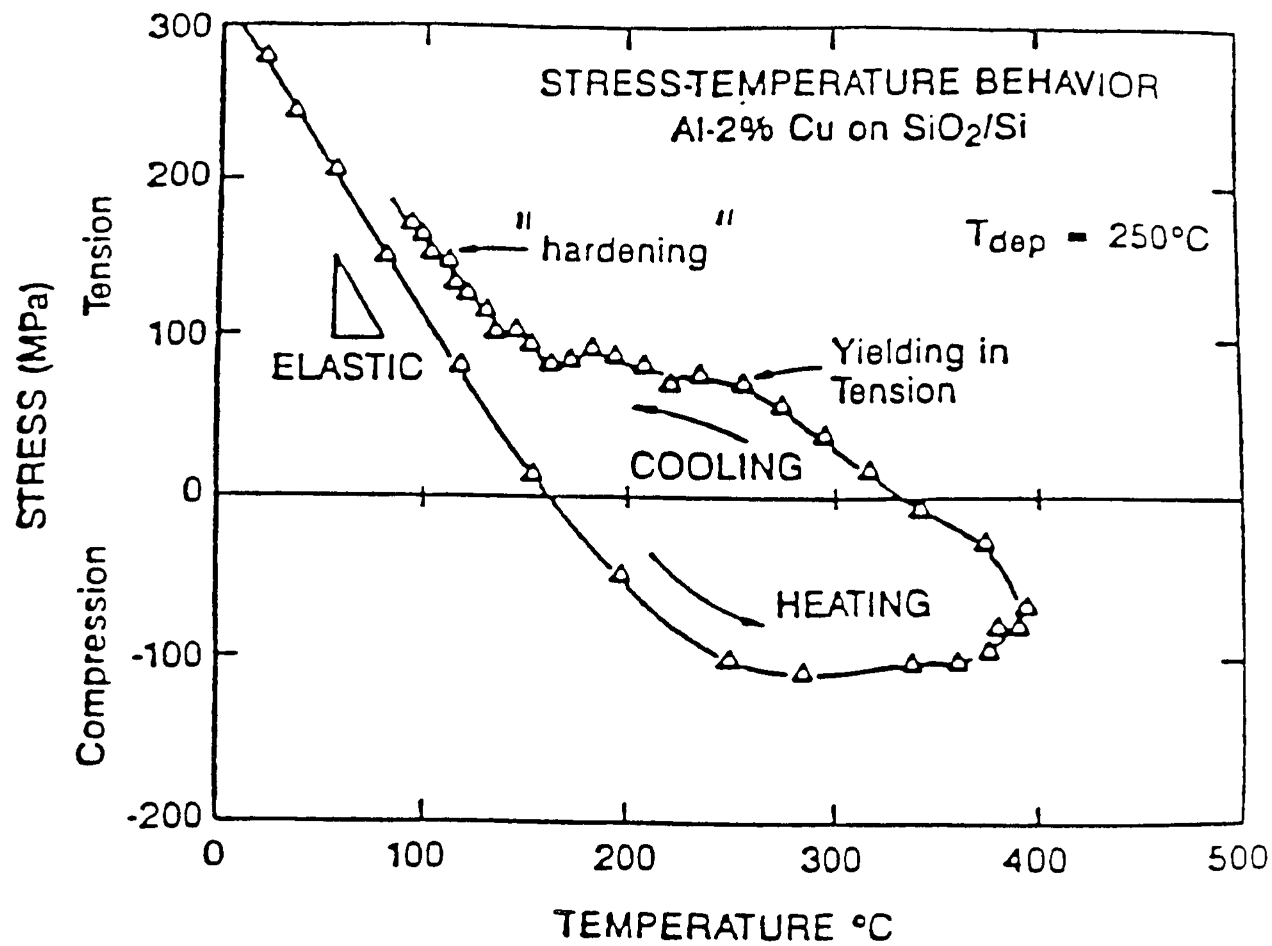

Figure 9. Stress-temperature behavior of Al-2% Cu on SiO_2/Si.

In general, Al films without passivation experience biaxial tension. However, after passivation deposition, most patterned metal films are under hydrostatic tension at room temperature because of the thermal coefficient of expansion mismatch for Al and the silicon nitride passivating layer: 23.5 vs. 2.2 ppm/°C.

The hysteresis loop of Figure 9 describes the σ vs. T characteristics of an "unpassivated" film. Heating to elevated temperatures (approximately 400°C) tends to reduce tensile stress in the alloy. In some cases, the stress can change its sense from tensile to compressive. Under compressive loading, the Al flows and relaxes (recovery) as it simultaneously undergoes recrystallization. During the cooling cycle, tensile stress begins to buildup in the Al film due to the differential contraction between the metal and substrate.

Hysteresis loops for Si_3N_4 encapsulated Al alloys have not been reported in the literature but will be presented in these studies. For continuous films, the nitride passivation does not have a large influence on the residual stress in the Al alloy; it does, however, have influence on the stress state.

3.9 Thin Film Stress Relaxation

For the purpose of this study, the activation energy and stress exponent were examined in the linear tensile region of the hysteresis loop, between room temperature and approximately 125°C (see Figure 9). The metallization failures of interest occur under these conditions. By studying thin film deformation with time in this regime, it is possible to extract kinetic information concerning the role of stress and temperature on the deformation of Al alloys. Higher temperature stress relaxation studies were also conducted.

For the stress relaxation experiments, the strain rate is not constant but can be evaluated by determining the slope of the stress vs. time curve at a constant temperature. Figure 10 shows a typical relaxation curve with the film stress decaying from an initial value of σ_o to a final value of σ_f. For this analysis, since the film strain is essentially fixed by the substrate, the strain rate is simply related to the stress decay rate by:

$$d\sigma/dt = d\epsilon/dt \cdot E_y \qquad [5]$$

where

$d\sigma/dt$ = instantaneous slope of the stress vs. time relaxation data

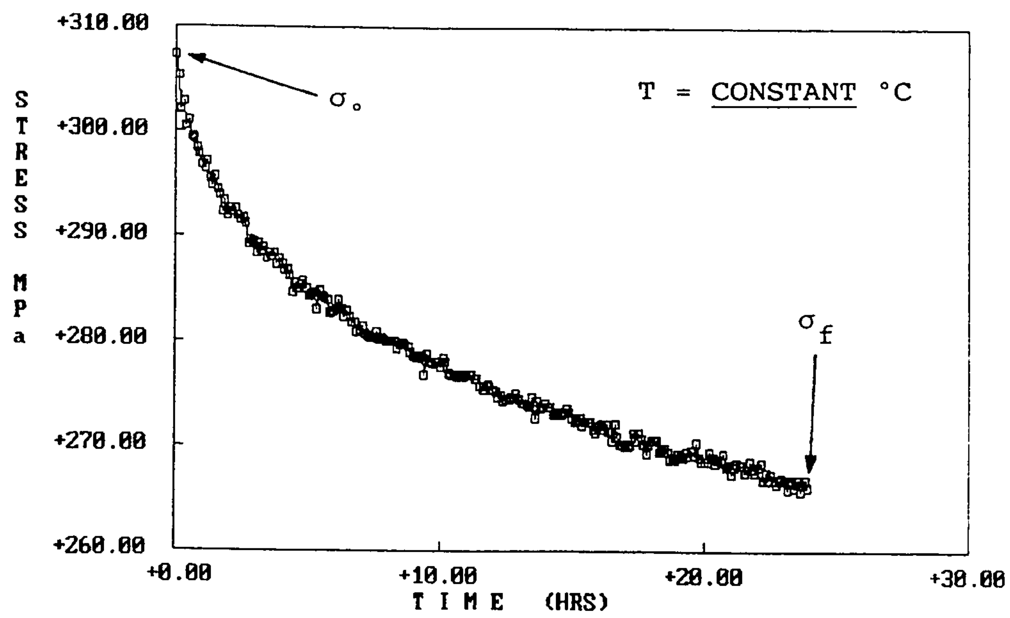

Figure 10. Characteristic stress relaxation curve.

E_Y = Young's Modulus at the temperature of the relaxation

Equation [5] and the standard creep relation (which will be shown later in eqn. [9]) can be combined to generate a relationship between the stress relaxation of a film, its stress and activation energy such that:

$$\ln [(d\sigma/dt)/D] = \ln A'' + \ln [(\sigma/E_Y)^n] \qquad [6]$$

To determine the value of the stress exponent, n, a ln-ln plot of $(d\sigma/dt)/D$ vs. (σ/E_Y) at constant temperature was extracted from the stress relaxation data. After evaluating the stress exponent, the activation energy E was obtained by rearranging equation [6] into the following form:

$$\ln [(d\sigma/dt)/(\sigma/E_Y)^n] = \ln (A''D_\circ) - \Delta E/kT \qquad [7]$$

A plot of $\ln [(d\sigma/dt)/(\sigma/E_Y)^n]$ vs. 1/T (Figure 11) should yield a straight line having a slope of $-\Delta E/k$.

By determining the dependence of deformation on stress and temperature for continuous thin films, a good foundation will be made for interconnect failure studies of the future.

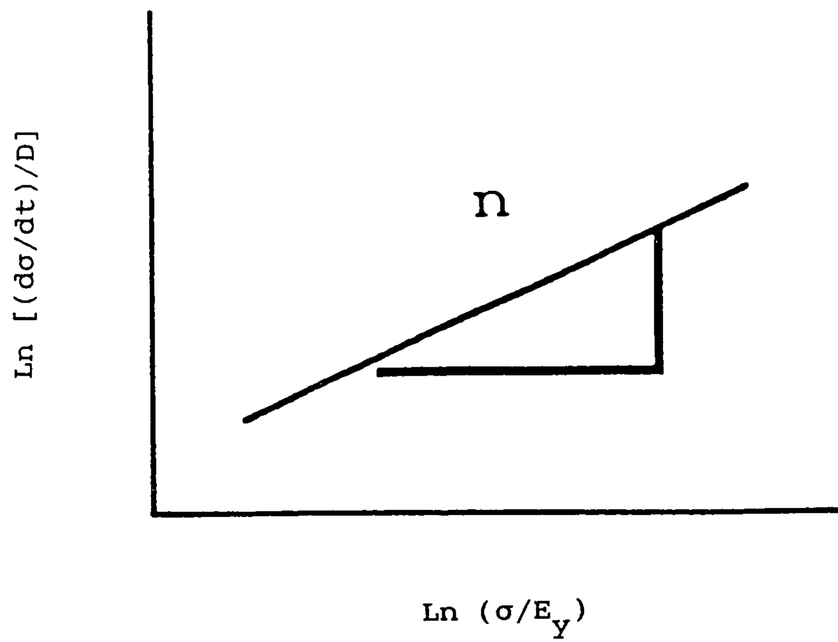

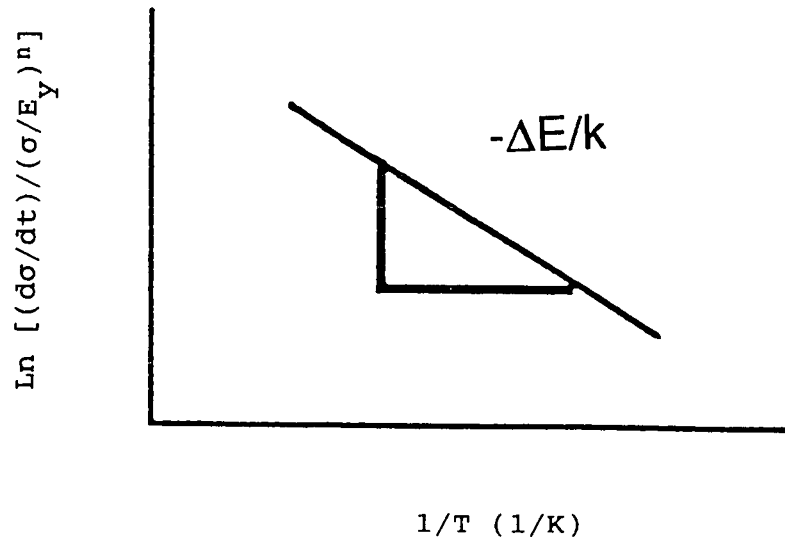

Figure 11. Plots to determine stress exponent and the activation energy from the stress relaxation experiments.

3.10 Metallization Line Failure

It is postulated that aluminum metallizations fail according to the following equation:

$$t_f = A\sigma^{-n} \exp(\Delta E/kT) \qquad [8]$$

where

t_f = The time to failure

A = Material constant dependent on grain size, texture and physical geometry

Since the creep deformation and relaxation properties of the metallization films are rationalized to govern patterned line failure, this work focussed on evaluating the activation energy and stress exponent from deformation/relaxation data for the sheet films. By determining these parameters, a relationship can be obtained that qualitatively tells us how resistant a material is to flow. However, the pre-exponential term of the failure relation, equation [8], is related to the grain size, distribution, and orientation. In order to determine the actual lifetime, patterned metal lines will have to be tested, in future experiments, to evaluate the pre-exponential term.

Since the failure time is inversely related to the strain rate $\dot{\epsilon}$, equation [8] can be modified and related to

the normalized creep relationship[21]:

$$\dot{\epsilon}/D = A' \ (\sigma/E_Y)^n \qquad [9]$$

where $\dot{\epsilon}/D$ is the strain rate divided by the diffusion coefficient, and A' is a structural constant dependent only on the operative failure mechanism.

3.11 Physical Significance of "n", The Stress Exponent

The magnitude of the stress exponent, described in equation [9], can tell a great deal about the mechanisms operative during stress relaxation. Pizzo[23] has reviewed the methodology used to relate the value of "n", which is typically called the power law exponent, to a specific creep mechanism. In previous discussions, it was observed that the stress exponent for Nabarro-Herring, Coble and dislocation creep never exceeds a value of above 5. Larger stress exponent values (approximately 10 and greater) are attributed to nonuniform stress and deformation in the body during testing. This effect has been observed in alloys with hard secondary phases, such a stainless steels[23] and dispersion strengthened materials[24]. In cases where polycrystalline films demonstrate large values of "n", it is plausible that local areas associated with "weaker" grain boundaries would undergo substantially

greater deformation than the surrounding neighbors. For Al alloys specifically, nonuniform deformation could also occur around secondary incoherent precipitates such as $CuAl_2$. A determination of the deformation uniformity will thus be implied from the relaxation characteristics of the Al alloys examined in these studies.

3.12 Deformation Maps of Ashby[25]

One final tool that can be used in the analysis of the stress relaxation data are the deformation maps of Ashby[25]. Figure 12 shows a map for Al having a grain size of 10 micrometers. The plot of the normalized shear stress vs. homologous temperature indicates the type of deformation mechanism one would expect to see under varying stress and temperatures. From this map, it appears that the Al alloys are in the transition region between the plastic flow and power-law breakdown. The experimental data of these studies will provide insight concerning the active mechanism for the observed deformation.

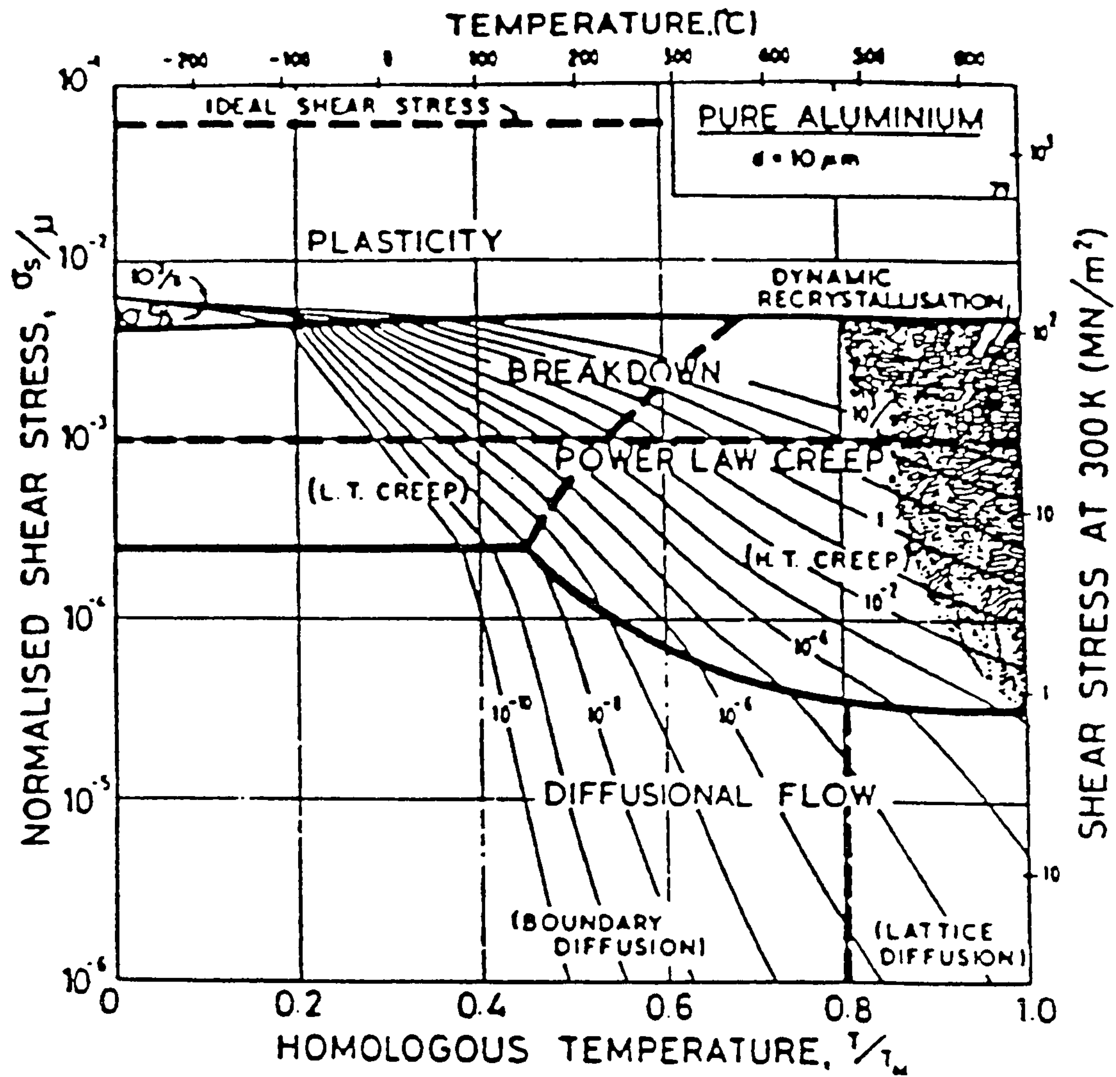

Figure 12. Deformation Mechanism Map of Ashby[25] for Al films having 10 micrometer grain size.

CHAPTER 4

EXPERIMENTAL

Aluminum alloy films were deposited onto thermally grown 5000Å SiO_2 films on 0.15 meter (100)Si substrates. The machine used for the deposition was a Varian 3290 sputter system which deposited films at a rate of approximately 167 Å/s. Films having a composition of Al -0.5%Cu-1.5%Si (by weight) were deposited at substrate temperatures of 25°C and 280°C, respectively. The Al alloy film thickness was fixed for all studies at 7500Å and was verified using diamond stylus profilometry, four-point probing and differential gravimetric measurements.

In order to evaluate the stress in the deposited films, a laser beam differential curvature technique was used. By using an optical scanning system* which could measure wafer curvature before and after the deposition of a film, the sign and magnitude of the stress could be determined. A schematic drawing of the curvature measurement technique is shown in Figure 13. This system has the unique feature of measuring the stress in a film during dynamic heating from room temperature to 500°C and was essential in the

---

* System was manufactured by Flexus, Incorporation, Sunnyvale, Ca.

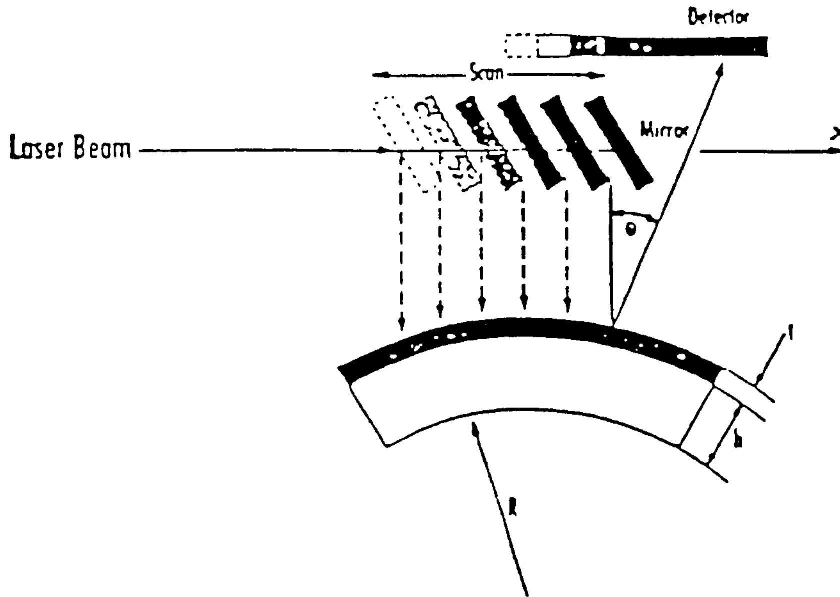

A substrate of thickness h, deformed to radius R by the film deposited on it.

$$\sigma = Eh^2/(1-\nu)6Rt \qquad [10]$$

where,

$E/(1-\nu)$	- The biaxial elastic modulus of the substrate (1.805E11Pa for 100 silicon wafers).
h	- Substrate thickness (m).
t	- Film thickness (m).
R	- Substrate radius of curvature (m).
σ	- The average film stress (Pa).

Figure 13. Schematic operational description of the optical scanning stress gauge used in these studies.

evaluation of Al alloy stress relaxation.

A series of stress vs. temperature hysteresis loops were generated for the Al films deposited under different conditions. Care was taken to "precondition" the alloy stress by placing the wafers through at least one hysteresis loop before conducting stress relaxation studies. After going through a complete cycle the stress vs. temperature characteristics were controllable and reproducible. Figure 14 shows the effect of preconditioning on the hysteresis characteristics of an Al alloy undergoing multiple stress cycling.

After determining the hysteresis characteristics of the Al alloy, stress relaxation studies were conducted. Isothermal stress relaxation was accomplished by arresting the cooling or heating ramp at a fixed temperature in the hysteresis loop. By doing this, two initial stress values were available at the same temperature for testing. The stress value obtained during cooling is always greater than that on the heating portion of the hysteresis loop when one considers an isothermal section. After selecting the desired temperature, the stress in the Al alloy was monitored as a function of time. These data could be retrieved and analyzed with the help of a software program resident to the stress gauge. Hysteresis studies

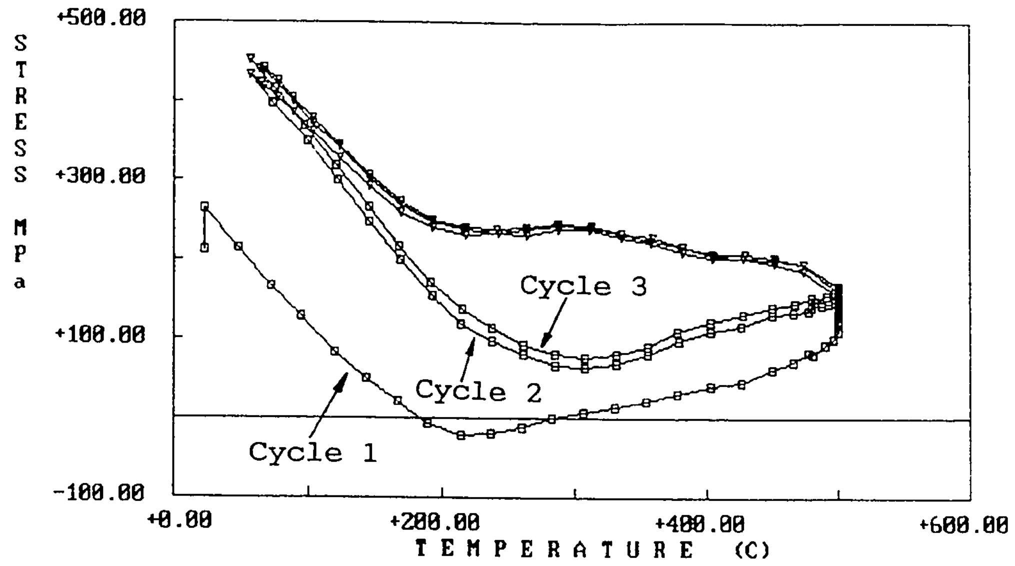

Figure 14. Series of hysteresis loops for an Al alloy showing the effect of preconditioning on stress reproducibility with temperature.

were performed in the temperature range between room temperature and 280°C. Stress relaxation studies were limited to the temperature regime of 40°C to 165°C to limit recovery and severely retard recrystallization in the Al alloys during testing.

Stress studies were also performed on dielectrics which are typically in intimate contact with interconnect alloys. Hysteresis tests were conducted to determine if dielectrics exhibited flow in the temperature regime of interest. Plasma Enhanced Chemically Vapor Deposited (PECVD) oxides and nitrides of silicon were evaluated. The silicon nitride films were deposited from a silane/nitrogen/ammonia plasma at 400°C in a PECVD reactor*. The deposited undoped silicate glasses used in this study were deposited from a silane/oxygen mixture at 400°C using a Concept I reactor**.

The hysteresis characteristics of these dielectrics were examined to see if they too would flow at elevated temperature. This effect would have to be accounted for when evaluating the Al stress in multilayered structures. The data obtained from the stress relaxation and hysteresis

---

* AMT 5000, Applied Materials Incorp., Santa Clara, Ca.

** Novellus Systems Incorp., San Jose, Ca.

loop studies were used to extract the stress exponent and activation energy associated with flow in the Al alloys.

CHAPTER 5

RESULTS AND DISCUSSION

5.1 General Overview of the Results and Discussion

Figure 15 summarizes the presentation sequence of the experimental results and discussion in this study. This flow also lists the background experiments conducted to investigate the nature of various films. From these results, the stress exponent and activation energy for the Al-Cu-Si metallization alloy were evaluated.

5.2 Stress vs. Temperature Hysteresis for Al Alloys

Figures 16 and 17 show the stress vs. temperature behavior of the Al-0.5%Cu-1.5%Si alloys deposited at substrate temperatures of 280°C and 25°C. The heating and cooling rates were approximately 4°C/min. The low initial value of tensile stress for the 25°C film occurs because this film did not undergo appreciable cooling after deposition. For the 280°C deposition, a large differential tensile thermal stress results.

In examining the initial thermal cycle data of both films, it is observed that tensile stress decays from room temperature to approximately 170°C. For further increases

EXPERIMENTAL RESULT TOPICS AND DISCUSSION

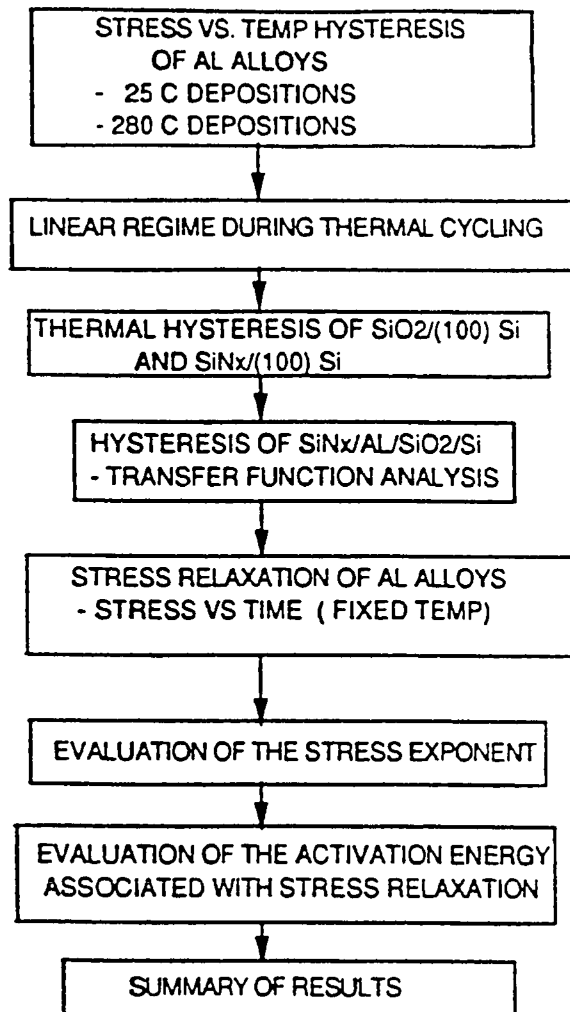

Figure 15. Experimental organization -- plan for analysis

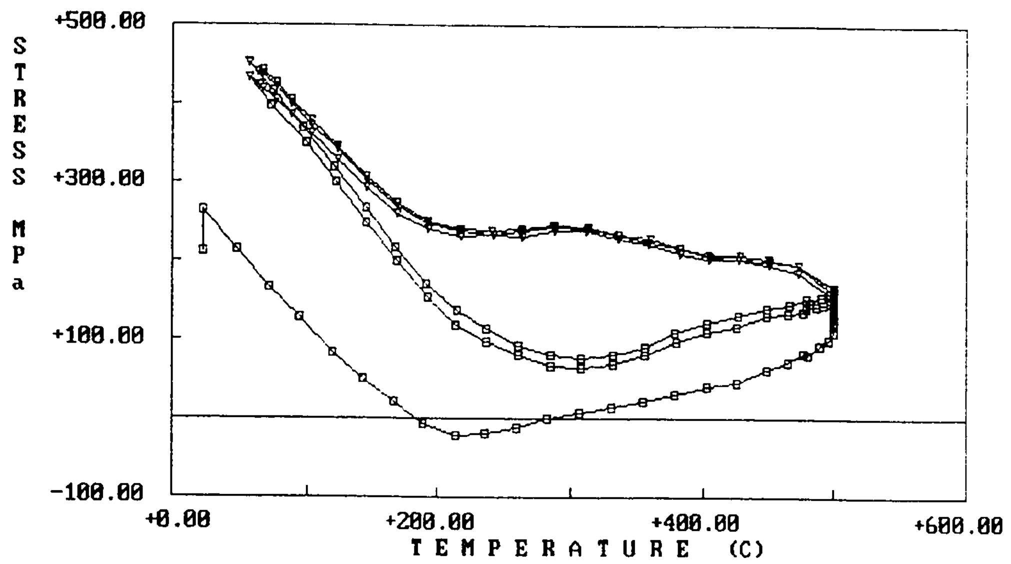

Figure 16. Stress vs. temperature hysteresis loop for an Al alloy deposited at a temperature of 280°C.

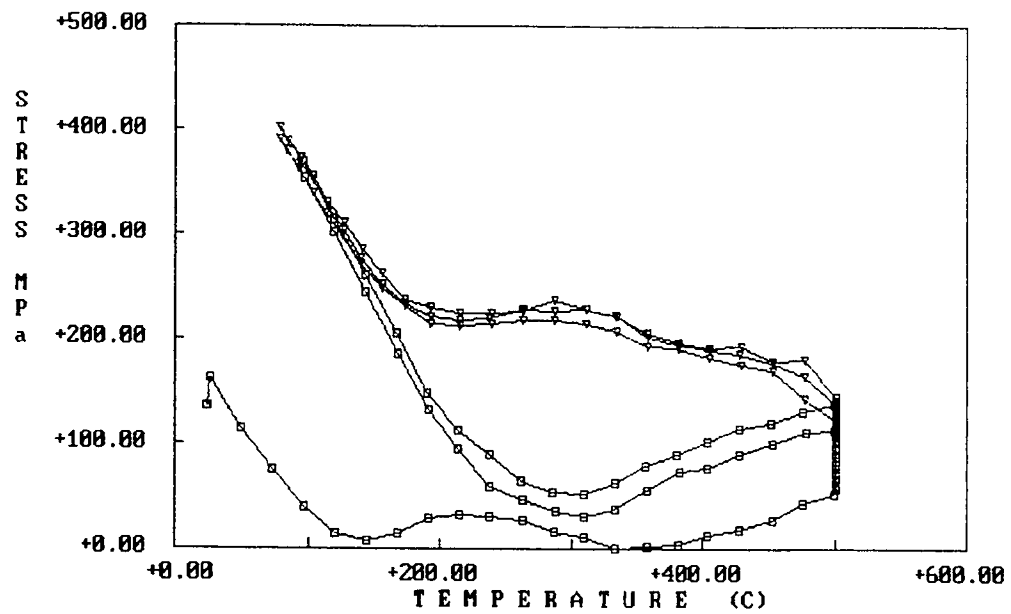

Figure 17. Stress vs. temperature hysteresis loop for an Al alloy deposited at a temperature of 25°C.

in temperature, the film deposited at 280°C continues to relax and actually becomes compressive as the temperature exceeds 180°C. As the temperature is increased, and after undergoing slight compressive stress, the 280°C deposited film surprisingly undergoes a tensile-going stress transition to 500°C.

The room temperature deposited film showed a more complex behavior. The stress fluctuated between 100°C and 300°C before also showing an increasing tensile stress component.

The above temperature-stress variations can be rationalized in terms of recrystallization and grain growth which reduces and densifies the deposited film. This densification process would support the buildup of a tensile stress in the film since the atoms, which collectively make it up, would occupy a smaller volume. At present, this increase in stress with higher temperatures is difficult to explain and the above interpretation is at best speculative.

After going through the first stress cycle (RT-500°C-RT at a rate of 4°C per minute), it was found that the final room temperature tensile stress was substantially higher than the as-deposited value for both films. Subsequent thermal cycles, however, resulted in reproducible hysteresis

loops (see Figures 16 and 17). Thus, the structural state of the metallization was considered to be reproducible in the analysis for any point on the hysteresis loop, if approached in the same heating or cooling sequence and rate, after the first complete cycle.

It is also interesting to note that the starting tensile stress at room temperature, after the first cycle, is essentially the same for both films. The data show that a single thermal cycle wipes out the prior strain history of the as-deposited Al film, due to competing strain hardening and relaxation events at high temperatures. Upon cooling, the thermal expansion coefficient difference between the substrate and metal film determines the room temperature tensile stress.

After one thermal cycle of a metallization film, the film is said to be "conditioned". The condition treatment was performed prior to each stress relaxation experiment, considered later in the presentation of results.

It should be pointed out here, that all subsequent stress relaxation data will represent the 280°C deposited Al alloy films.

5.3 Linear Thermal Deformation Region for Al Alloy Thin Films

Figure 18 shows a stress vs. temperature cycle for an Al alloy metal film conditioned between room temperature and 120°C. For moderately short cycling times (approx. 2 hrs per cycle), the stress loop is very tight and reproducible. Figure 19 shows the corresponding cyclical nature of the a) temperature with time and b) stress with time for a typical thermal excursion. A large degree of relaxation is not seen in these data since the tensile stress is low ($<$ 100 MPa) at the high temperature end of the stress cycle; and, the high-end temperature is only 120°C. In addition, for the cycle represented in Figure 9, films did not sit at a fixed elevated temperature before cooling was initiated. It would be expected, and will later be observed, that time dependent material flow does occur over longer time intervals for these films, which are under substantial tensile stress. For a frequency of 0.5 cycles per hour, reversible behavior occurs at temperatures up to 160°C for the Al films of this study.

5.4 Thermal Hysteresis of SiO_2/(100)Si & SiN_x/(100)Si

Since the Al alloy used in this study is to be encapsulated between PECVD dielectrics of SiO_2 and SiN_x,

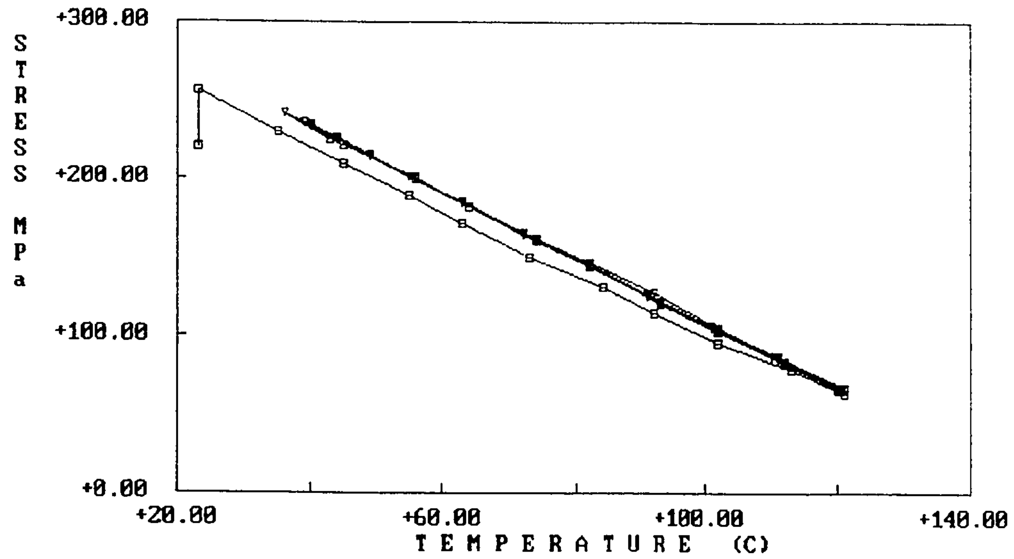

Figure 18. Stress vs. temperature characteristics for an Al alloy deposited at 280°C. Films exhibited a linear decay in tensile stress with temperature at a heating rate of approximately 95°C/hour.

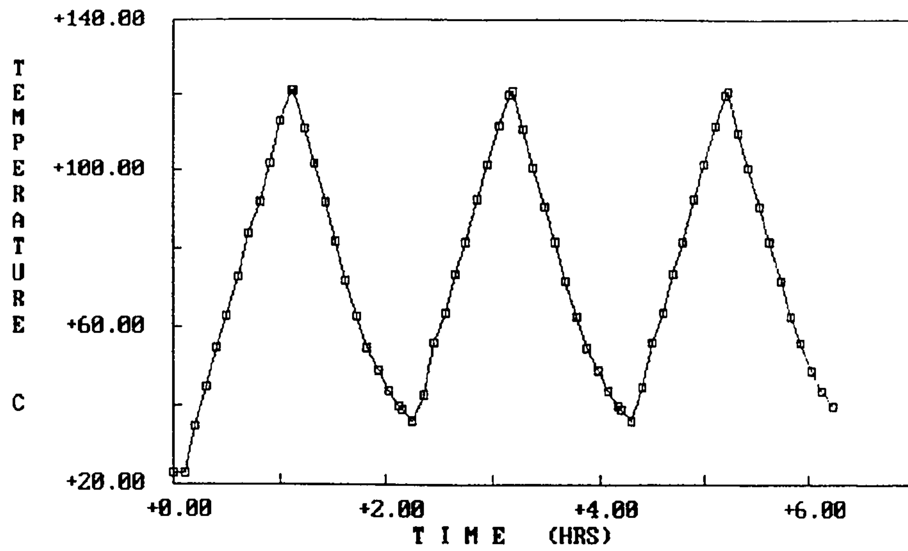

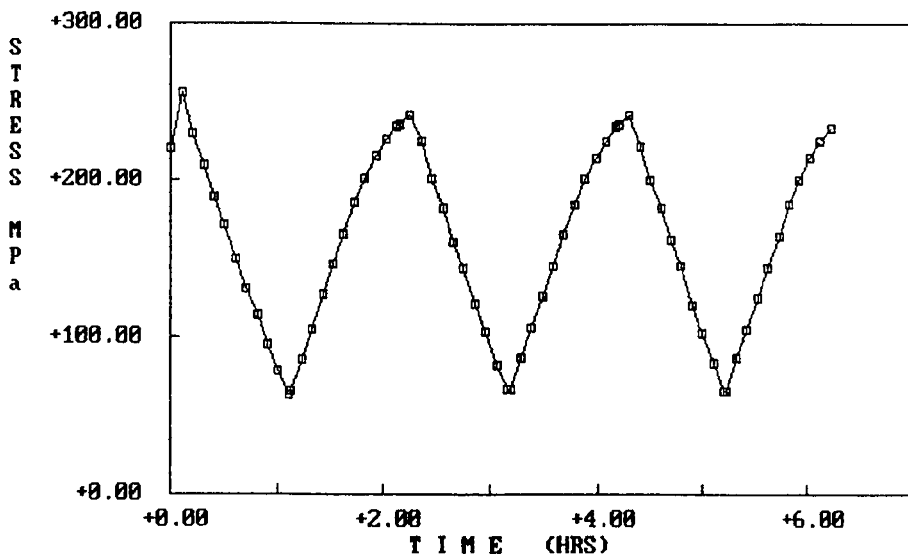

Figure 19. Cyclical data for the linear stress vs. temperature region shown in Fig. 15. The heating and cooling rates were approximately 90°C/hour.

it is important that the relaxation kinetics of these dielectric films are also understood. Stress versus temperature plots for the dielectrics used in this study are shown in Figures 20 and 21.

Figure 20 shows the stress hysteresis loop for a PECVD SiN_x film on (100) silicon. This film was deposited in a AMT 5000 reactor at 400°C. For the conditions of the deposition, the film had a small initial compressive stress ($< -5 \times 10^7$ Pa). After one thermal cycle, a slight adjustment towards tensile stress occurs in the film. Upon further cyclic heating between room temperature and 500°C, little if any stress change occurs. This is due to the close match of the expansion coefficients of the Si substrate and the SiN_x film. In examining the small area swept out in this hysteresis loop, little if any film deformation energy is released. Although large stresses were not generated in the nitride for these studies, it is well known that silicon nitride is a strong material which undergoes little, if any, plastic deformation at the moderate to low homologous temperatures of this study (0.2 T_m). It is no wonder that the constraint on patterned Al alloys, imposed by the SiN_x film, is large during differential cooling and can adversely affect metal reliability.

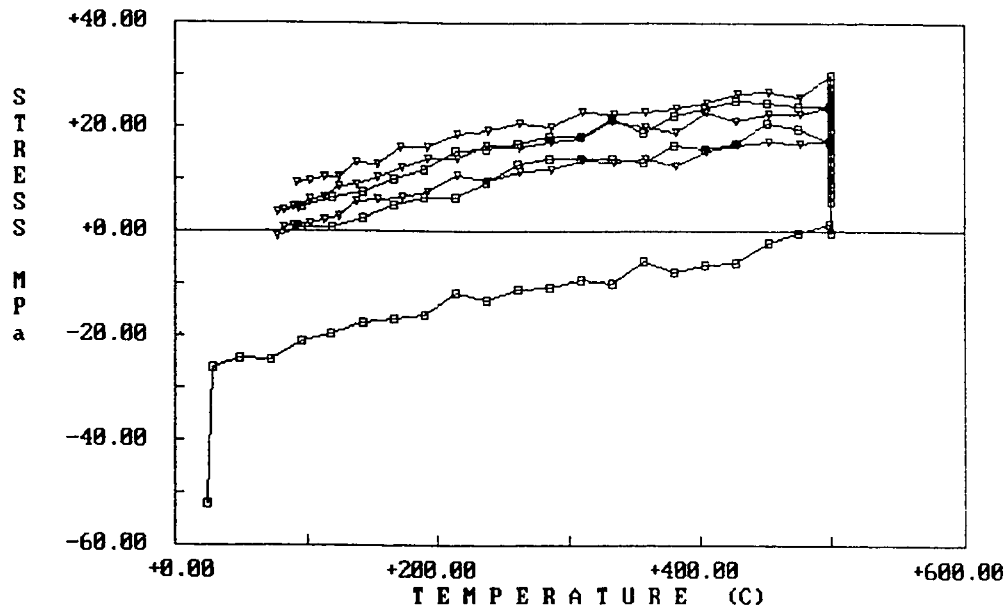

Figure 20. Stress hysteresis loop for SiN_x cycled between room temperature and 500°C at a rate of 225°C per hour. The film exhibited little plastic flow during this process.

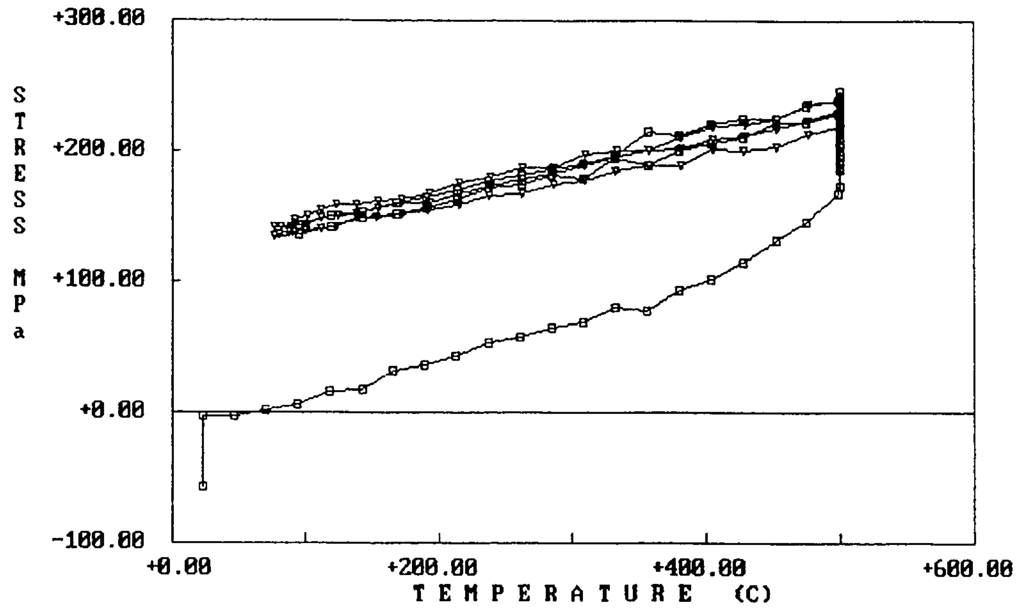

Figure 21. Stress hysteresis loop for PECVD SiO_2 deposited at 400°C. The films were cycled at a heating rate of 238°C per hour.

Figure 21 shows the stress versus temperature characteristics of an undoped PECVD SiO_2 film on a (100)Si substrate. This film was deposited in a Novellus Concept I reactor at 400°C at an average rate of 1 micrometer per minute. Like the SiN_x dielectric, the oxide retained a small compressive stress after deposition. However, during the first hysteresis cycle, a large shift towards tensile stress is seen.

It is well known that deposited oxides can absorb and retain atmospheric moisture during room temperature exposure. This incorporation of water requires that a compressive stress build up in the oxide, since more molecules are being "stuffed" in the same volume. Upon heating to 500°C, this water is probably desorbed from the oxide with an accompanying increase in tensile stress. Although the slope of the stress versus temperature plot is small, the curve indicates a slightly larger mismatch between the PECVD oxide and the Si substrate in comparison to the nitride. In both cases, however, the expansion coefficients are well matched in comparison to the Al metallization.

5.5 Hysteresis of $SiN_x/Al/SiO_2/(100)Si$ - The Transfer Function

In order to study the stress relaxation of Al films with an overlying passivation, studies were conducted to determine the component of Al stress present in a compound multilayer structure. Figure 22 shows the hysteresis loops of two identical Al alloy films, except that one is encapsulated by a continuous SiN_x film. The other film has a free surface. It has be shown by Nix[16] that continuous Al films see little effect from the overlying passivation layers. A mechanical analysis of a Si substrate with an Al film covered with a nitride passivation layer shows that the stress change in the Al due to the passivation can be expressed by the following equation:

$$\sigma_{Al} = - 3 \, t_p/t_s \, \sigma_p \qquad [11]$$

where

σ_{Al} = stress change in the aluminum due to the overlying passivation

σ_p = stress in the nitride film as deposited

t_p = thickness of the nitride layer

t_s = thickness of the substrate

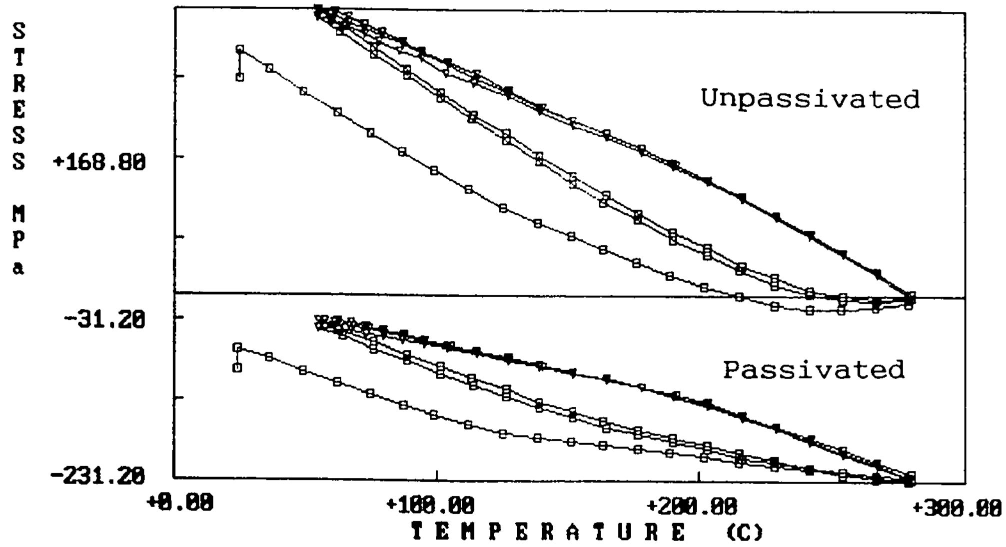

Figure 22. Hysteresis loops of Al and SiN_x coated Al thin films used to obtain the transfer function. Both films were heated at approximately 128°C/hour.

Since the thickness of the substrate is much greater than the passivation film, it is seen from equation [11] that the stress change in Al caused by the passivation is small. This equation indicates that the Al and nitride impose little stress on one another for the continuous film situation. When Al is pattered into very small features, this would not be the case.

A one-to-one mapping was performed to generate a transfer function capable of extracting the Al stress from the SiN_x encapsulated multilayer film. This was accomplished by directly comparing the Al and nitride stress values of the two different structures at a fixed temperature for the heating and cooling portions of the hysteresis curves. This exercise was performed on nine different sets of hysteresis data to generate a statistical correlation. For the 280°C deposition conditions and a maximum hysteresis temperature of 280°C, a simple linear regression analysis was used to generate the transfer function:

$$\sigma_{Al} = 4.0138 \text{ X } 10^{8} + 1.8871\ \sigma_{SiN_x} \qquad [12]$$

where

σ_{Al} = calculated Al stress in the composite film in Pascals

σ_{SiN_x} = Measured stress of the composite film with SiN_x

The plot of the master transfer function that was used to derive this expression is shown in Figure 23. It should be pointed out that the correlation between data was excellent with a correlation coefficient of 0.986. This function smoothly transforms the stress of the multilayered SiN_x film curve to one describing the Al film stress.

Although this derivation was performed as a function of temperature and not time, was assumed that the stress mapping between free Al and SiN_x covered films was independent of both variables. In the present analysis, the function was used to extract stress relaxation curves for Al from films having a SiN_x top layer.

Figure 24 shows the excellent correlation of stress relaxation data for a freely exposed Al film vs. one encapsulated with SiN_x. These two film types were tested under identical conditions. Except for a 1 X 10^7 Pa offset, the directly measured and calculated Al alloy stress vs. time data from the freely exposed and SiN_x encapsulated Al films are essentially identical.

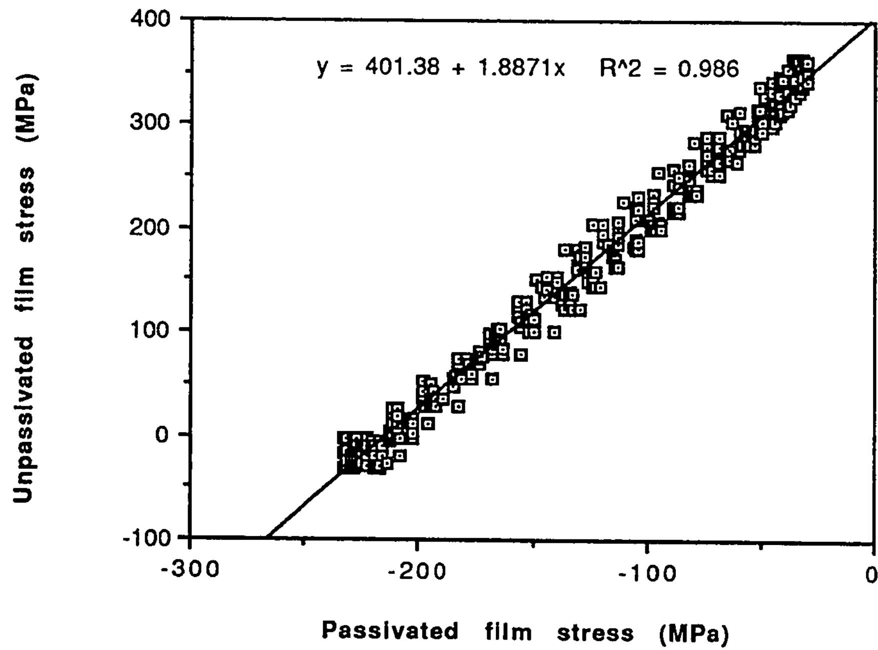

Figure 23. Plot of the master transfer function relating the Al thin film stress in free vs. SiN_x encapsulated thin film structures.

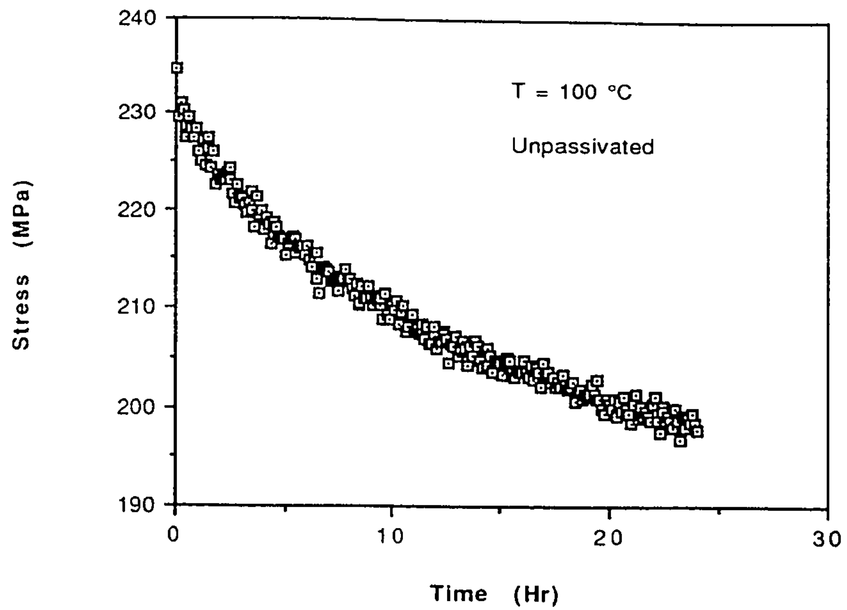

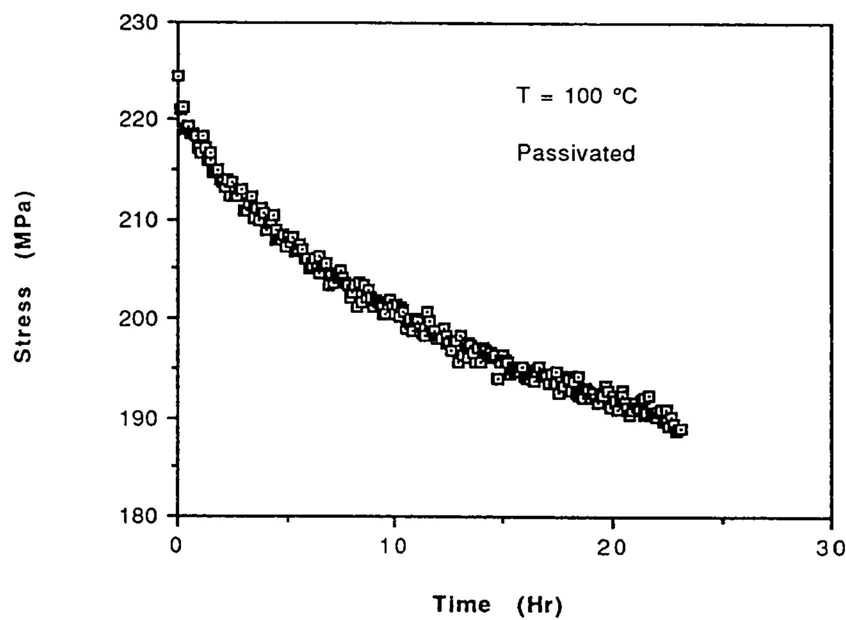

Figure 24. Measured and extracted Al alloy stress relaxation curves for thin films without and with a SiN_x passivation layer. The agreement between the two data sets was excellent.

5.6 Experimental Stress Relaxation Studies

Stress relaxation data were taken for Al films at different initial stresses and temperatures. Tables 1 and 2 contain a summary of polynomial expressions used to fit the stress relaxation data for Al films deposited at 280°C. Figure 25 is a plot of the stress vs. time for the unpassivated films of this study. It was interesting that the data could not be cleanly fit with an exponential function having a single parameter. If the long time portion was fit with a single valued exponential, it was observed that a greater than expected stress decay occurred for short times. This indicated a "fast" initial deformation process was occurring in all of the films. More will be said about this phenomena after analyzing the value of the stress exponent.

5.7 Evaluation of the Stress Exponent from Experimental Stress Relaxation Data

The stress exponent [equation (8)] was determined using a self consistent approach which is outlined in Figure 26. The first step was to take the published grain boundary diffusion coefficient data[26] and calculate the diffusivity for each temperature of the stress relaxation tests. To check the validity of using the grain boundary

Table I. Summary of Al-0.5% Cu-1.5% Si Stress Relaxation Data		
Stress (t) = a + bt + ct^2 + dt^3 + et^4 + ft^5		
Wafer I.D.	Test duration (Hrs)	Initial Stress (MPa)
121	23.9	339
118	23.9	307
131	72.4	321
119	23.9	300
140	8.5	289
130	24	235
128	23.9	239
129	24	176
120	23.8	181
122*	23.1	224
123*	24	249
125*	24	265
124*	24	197
*Extracted from SiNx/Al/SiO2/Si data using transfer function		

Table 1. Summary of initial test conditions and test duration for stress relaxation tests on Al films deposited at a substrate temperature of 280°C.

Table 2. Summary of Al-0.5% Cu-1.5% Si Stress Relaxation Data							
Stress (t) = a + bt + ct^2 + dt^3 + et^4 + ft^5 (MPa)							
Wafer I.D.	Temp (C)	a	b	c	d	e	f
121	40	336060000	-7044000	957130	-74859	2851.5	-41.355
118	51	304050000	-6954700	902310	-69351	2615.8	-37.729
131	70	312570000	-4522400	213570	-5587.5	70.413	-0.33657
119	75	296950000	-9243700	1241900	-98354	3810.6	-56.14
140	100	288680000	-17782000	5385500	-1102300	115710	-4726.5
130	100	231170000	-4302300	397360	-25929	890.76	-12.026
128	120	233920000	-10734000	1588300	-125980	4800.1	-69.45
129	120	175210000	-2622500	277900	-18364	615.88	-8.0712
120	165	178930000	-7138600	969100	-76814	2953	-42.772
122	100*	221650000	-4505500	513390	-41732	1735.6	-27.708
123	124*	243080000	-11284000	1525700	-114140	4187	-58.934
125	137*	261520000	-12300000	1886100	-147500	5517.7	-78.36
124	150*	189490000	-8441100	1343900	-110220	4322.3	-64.288
	*Extracted from SiNx/Al/SiO2/Si data using transfer function						

Table 2. Summary of polynomial expressions used to fit the stress relaxation data for Al films deposited at a substrate temperature of 280°C (See Table 1).

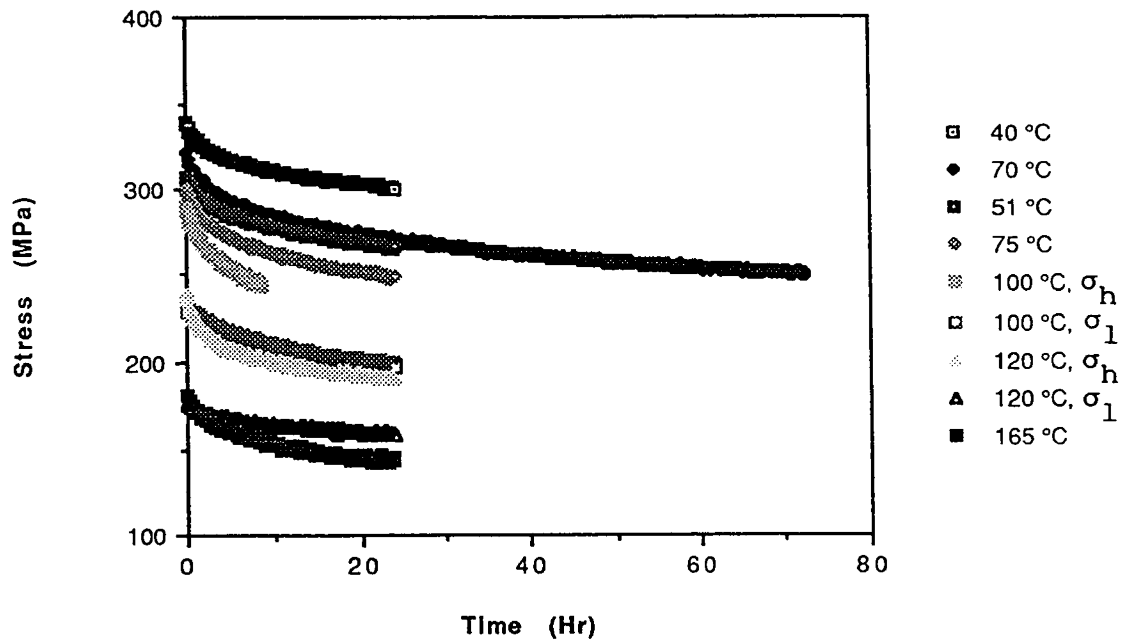

Figure 25. Stress relaxation data for all nonpassivated Al alloys deposited at 280°C.

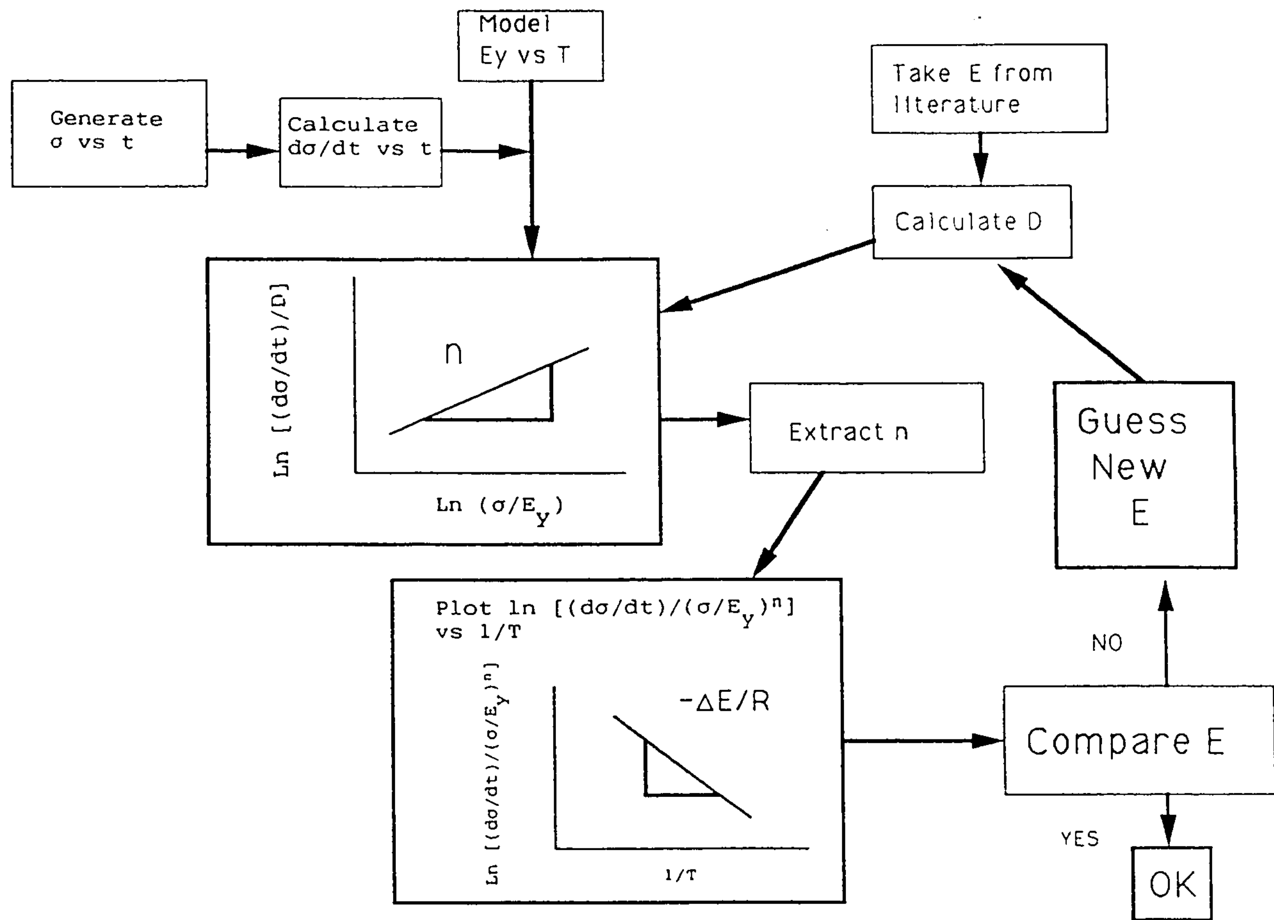

Figure 26. Method for the evaluation of the stress exponent and activation energy.

activation energy for all experiments, a plot of the lattice and grain boundary diffusivity versus reciprocal temperature was generated (Figure 27). This plot takes grain size effects into account and establishes the temperature where a change in mechanism to lattice diffusion dominated transport would be expected. From Figure 27, it was determined that grain boundary diffusion is the dominant mechanism to approximately 0.8 of the melting point of aluminum for fine grained (grain size = 32 micrometers) materials. Lattice diffusion does not play a great role in the stress relaxation.

The grain boundary diffusion activation energy of Ashby[26] was used to estimate the diffusion coefficients for the analysis of n, the stress exponent. The temperature dependent elastic modulus from McClean et al[22], described in section 3.7, was also used in the interpretation of the data.

The second step in determining the stress exponent involves a logarithmic analysis of the stress relaxation data obtained in this experiment. Figure 28 presents the data for all films examined in this study. A fit through the data of all curves indicates a stress exponent of approximately 9.0. The correlation was quite good (0.883) for the collective data set. Most of the curves

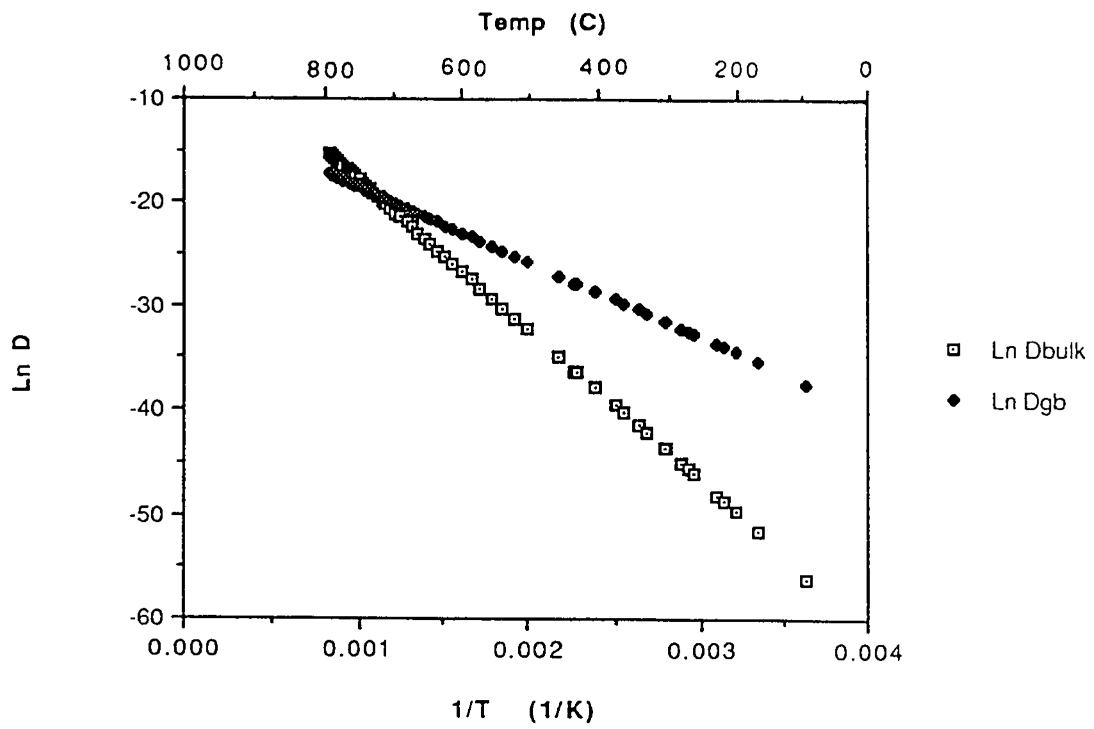

Figure 27. The Grain boundary and lattice diffusion coefficient of pure aluminum versus reciprocal temperature [From data of Ashby[26]].

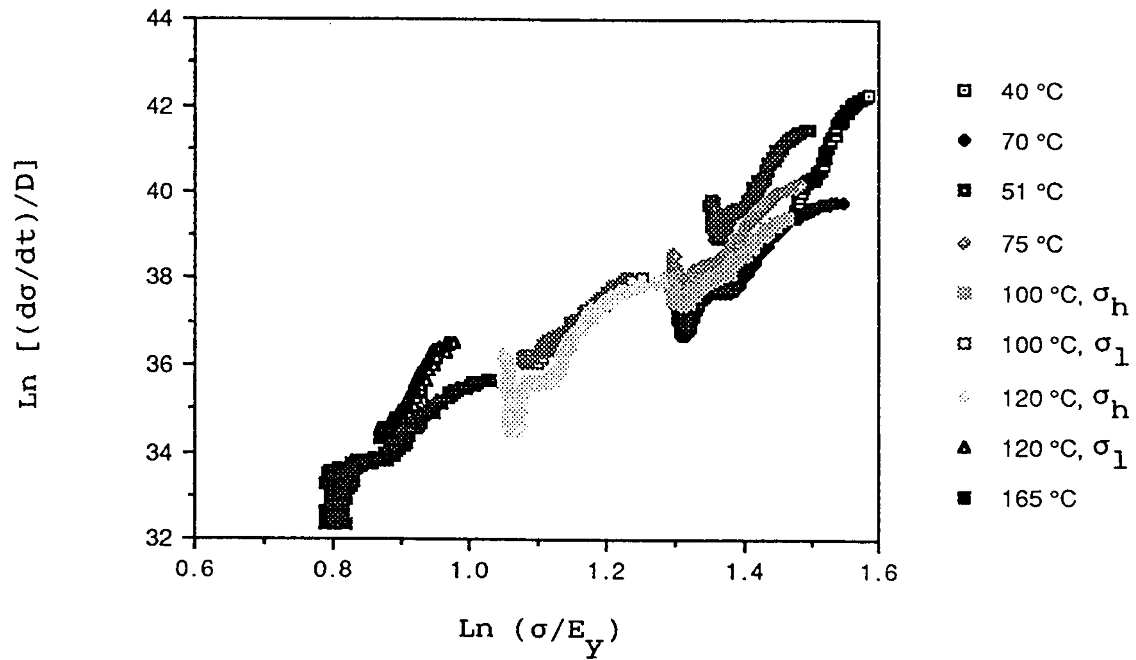

Figure 28. Ln-Ln plot of the $(d\sigma/dt)/D$ versus (σ/E_Y) for all films used in the stress relaxation studies.

demonstrated the same "s-like shape" which can be explained by number of complex parallel processes of progressively lower stress dependence as the stress is relaxed. The final analysis of the data will attempt to explain the expected shift in slope during the stress relaxation process.

5.8 Self Consistent Evaluation of the Activation Energy

To self consistently check whether the assumed activation energy of the relaxation process was correct, a semilog-plot of $[(d\sigma/dt)/(\sigma/E_y)^n]$ vs. $1/T$ was generated as was described in Section 5.7. The data are shown in Figure 29. A linear regression analysis of the data yields an activation energy of 13,700 cal/mole. This value is in excellent agreement with the grain boundary activation energy of 14,400 cal/mole of Ashby[26] that was used to extract the stress exponent. It is also consistent with the activation energy reported for Al electromigration[27-28]. The correlation coefficient for this data analysis (0.868) supports the hypothesis that the stress relaxation process is dominated by grain boundary diffusion.

5.9 Overall Perspective of the Al Thin Film Relaxation

From the stress vs. time behavior of Al-0.5%Cu-1.5%Si films at various temperatures, the following picture will be

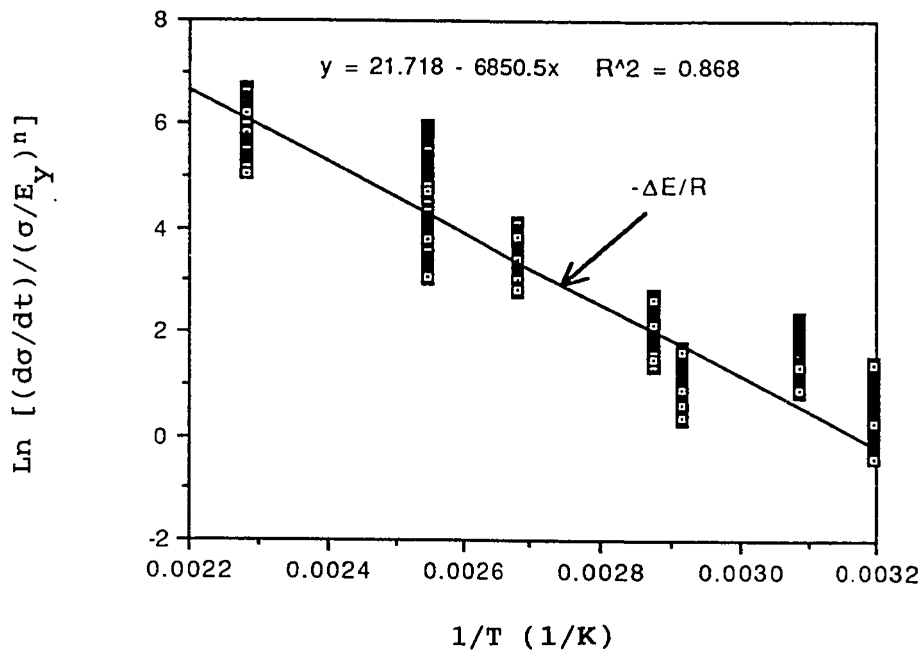

Figure 29. Extraction of the activation energy for grain boundary diffusion from a semilog plot of the $\ln [(d\sigma/dt)/(\sigma/E_y)^n]$ versus reciprocal temperature.

postulated concerning the relaxation process in these materials:

(1) In the initial phase of stress relaxation, the rate of stress decay is greater than would be expected from a process with a single deformation mechanism.

(2) The large stress exponent associated the relaxation process suggests a highly nonuniform stress and deformation distribution in the material.

(3) The average activation energy of the process (approx. 13,800 cal/mole) is essentially identical to reported values for grain boundary diffusion (14,400 cal/mole) by M. F. Ashby(26). These data indicate that whatever the active deformation mechanism is, it is associated with the rearrangement of atoms in the grain boundary regions.

(4) For the low temperatures examined in these studies, recrystallization should not be occurring during the isothermal stress relaxation tests. This can be inferred from the bulk data presented in Section 3.7.

(5) Thermal cycling of the Al alloy "pumps up" the material with mechanical free energy. Upon heating the material

to high temperatures (i.e., T ≥ 175°C), the yield stress is low and recovery, accompanied possibly by grain growth, occurs. At practical alloy temperatures of 450°C, most of this free energy is released by internal atomic rearrangement, only to be restored during the cool-down to room temperature. However, during cooling the material strengthens and a large tensile stress builds in the Al alloy due to differential expansion differences with the substrate. For alloys deposited at different temperatures, most see similar room temperature tensile stress after one hysteresis cycle up to 450°C. At room temperature, this large amount of mechanical energy is available to induce time dependent flow and the flow occurs preferentially at grain boundaries.

In light of these results, the following model will be proposed to explain the observations made in this study.

Polycrystalline Al films have grain boundaries exhibiting a distribution of activation energies based on their growth orientation with respect to one another. This variation occurs because the mismatch between growing grains generates different amounts of free volume in the boundary region. In turn, this free volume is related to the average number and strength of bonds between atoms in this

disordered region. It is proposed that there is a distribution of activation energies about an average value based on statistical variations in the individual boundaries. During the initial phase of stress relaxation, the regions having the lowest activation energies for rearrangement in the distribution will account for most of the deformation seen in the alloy. (Conversely, these areas have the highest free energy due to their high degree of non-bonding in the grain boundary itself). As this process occurs, stress reduction by rearrangement proceeds more rapidly than expected and accounts for a highly local deformation in the macroscopic film.

A similar model can be constructed if one looks at the grain boundary region as one consisting of a pileup of dislocations. By rearrangement of the boundary to a lower energy state, dislocations, through climb processes, can give up large amounts of vacancies into the boundary itself. This accelerates the local deformation process. However, the process slows as the mechanism of transport and flow lowers the free energy of the boundary and other adjacent grains rotate to accommodate the material rearrangement. <u>This rapid local deformation is inferred from the large stress exponent seen in these studies.</u>

This model is also consistent with the activation

energy associated with a grain boundary diffusion process. As the local driving force in these higher energy grain boundaries drops, the deformation becomes more characteristic of the whole distribution. Since more grains can equitably carry the thermally generated stress, the rate of stress relaxation is reduced.

This process can be repeated by taking the film and placing it through a high temperature hysteresis cycle which "pumps" the polycrystalline film with more mechanical free energy upon cooling to room temperature. Upon arresting the film at the same temperature, a similar relaxation process would be expected to occur but would not have to involve the same identical grains which rapidly slipped in the first relaxation process. Since we have a distribution of grains which accommodated the deformation in the first cycle, grains that rotated during the accommodation process may become the "fast deformers" due to their new orientation. The differential stress generated during cooling can increase the "effective" dislocation density in grain boundary regions of the thin film due to the presence of Frank-Reed sources. If accommodation does not occur rapidly in local areas of the film, flow divergences responsible for void or crack formation would be expected in the alloys.

It is of great practical-importance to know what

fraction of the grains are involved in the stress relaxation observed in these studies. From the data, it was estimated that approximately 10 to 15% of the total strain energy is released during a single relaxation cycle. It would be interesting to see if any "weak" grain boundary region had exceeded its local critical elongation limit. For thin films with many grains, elongation is a statistical property which requires the collective movement of all grains during macroscopic deformation (accommodation).

This situation poses a number of important questions that must be addressed concerning patterned metal lines. Presently, the situation exists where the linewidth is smaller than the average grain size of the film! For fine line interconnects, it is probably correct to talk about a critical "energy-distortion limit" of a single grain boundary. When this limit is exceeded, slit or wedge-shaped cracks would result. This appears to be a reasonable assumption, since the boundary is not accommodated by the rest of the grains in the film, as would be the case for continuous films.

The concern here is not with large area thin films having substantial numbers of strain accommodating grains; but with patterned metal lines having possibly only one grain boundary across the line width. Since accommodation

is not available to these fine lines, the stress exponent of a series of these lines would be expected to be substantially higher than that of a thin continuous film. This would occur due to the highly localized deformation at the grain boundary. During thermal cycling, certain grains may see the same repetitive stress relaxation, time and again, leading to accelerated failure. If this model is correct, there may be some disappointing reliability issues facing the interconnect engineer using Al alloys for submicron interconnects.

CHAPTER 6

CONCLUSIONS

In these studies, a number of interesting properties of thin Al-0.5%Cu-1.5%Si alloys were extracted from stress relaxation experiments.

They are as follows:

(1) A transfer function was generated which allowed the extraction of the Al film stress from a multilayer thin film having an overlying passivation.

(2) For the initial stage of stress relaxation, the rate of stress decay is greater than from a process having a single decay constant.

(3) The large stress exponent obtained for these films ($n = 9$) suggests that the deformation associated with the relaxation process is highly nonuniform. It is expected that a small fraction of the grains in the film slip rapidly and account for a majority of the deformation occurring in the initial stages of stress relaxation.

(4) The activation energy calculated from the stress

relaxation data appears to be associated with the diffusion of vacancies in grain boundaries. The activation energy of 13,800 cal/mole is in excellent agreement with the reported value of 14,440 cal/mole[26].

(5) Thermal cycling of the Al alloy "pumps up" the material with mechanical free energy which is used to drive the relaxation process.

(6) It is rationalized that accommodation, which is present in the continuous Al alloy films, may not be available with fine metal interconnects having grain sizes larger than the linewidth. This issue may have highly adverse reliability implications for fine line interconnects.

The results obtained in this study provide valuable insight into the stress and temperature dependence of relaxation in Al alloy films. In future experiments, the patterning of these films will help to define the role film geometry, grain size and texture play in stress induced failure. It is expected that grain boundary diffusion will be the mechanism responsible for failure, with material rearrangement occurring under triaxial stress. Growing voids or cracks should become more likely as "weak" non - accommodated grains undergo highly localized deformation.

REFERENCES

1. van de Ven, E.P.G.T., "Plasma Deposition of Silicon Dioxide and Silicon Nitride Films", Solid State Technology, (April 1981), pp. 167-171.

2. Mayumi, S., Umemoto, T., and Shishino, M., "The Effect of Cu Addition to Al-Si Interconnects on Stress Induced Open-Circuit Failures", IEEE/IRPS, (1987), pp. 15-21.

3. Nix, W.D., Materials Science and Engineering 207B (Mechanical Properties of Thin Fims) lecture notes, Stanford University, (1988), p. 154.

4. Owada, N., Hinode, M., Horiuchi, K., and Mukai, K., "Stress induced Slit-Like Void Formation in a Fine Pattern Al-Si Interconnect During Aging Test", Proceedings of Second International Multilevel Interconnect Conference, Cat. # 85ch2197-2, (1985), pp. 173-179.

5. Hinode, K., Owada, N., Nishida, T., and Mukai, K., "Stress Induced Grain Boundary Fractures in Al-Si Interconnects", J. Vac. Science and Tech., B5(2), (Mar/April 1987), pp. 518-522.

6. McPherson, J.W., and Dunn, C.F., "A Model for Stress Induced Voiding in Very Large Scale Integrated Al-Si(1%) Metallization", J. Vac. Science and Tech., B5(5), (Sept/Oct 1987), pp. 1321-1325.

7. Groothuis, S.K., and Schroen, W.H., "Stress Related Failures Causing Open Metallization", IEEE Proceedings of the 1987 International Reliability Physics Symposium (IEEE/IRPS), (1987), pp. 1-8.

8. Yue, J.T., Funsten, W.P., and Taylor, R.V., "Stress Induced Voids in Aluminum Interconnects During IC Processing", IEEE/IRPS, (1985), pp. 126-137.

9. Hinode, K., Asano, I., and Homma, Y., "Mechanism of stress-induced Migration", IEEE/V-MIC Conf., (June 13-14, 1988), pp. 429-435.

10. Yost, F.G., Amos, D.E., and Romig, A.D. Jr., "Stress-Driven Diffusive Voiding of Aluminum Conductor Lines", IEEE/IRPS, (1989), pp. 193-201.

11. Klema, J., Pyle, R. and Domangue, E., "Reliability Implications of Nitrogen Contamination During Deposition

of Sputtered Aluminum/Silicon Metal Films", IEEE/IRPS, (1984), pp. 1-5.

12. Curry, J., Fitzgibbon, G., Guan, Y., Muollo, R., Nelson, G., and Thomas, A., "New Failure Mechanisms in Sputtered Aluminum-Silicon Films", IEEE/IRPS, (1984), pp. 6-8.

13. Herschbein, S.B., Zulpa, P.A., and Curry, J.M., "Effect of Silicon Inclusions on the Reliability of Sputtered Aluminum-Silicon Metallization", IEEE/IRPS, (1984), pp. 134-137.

14. Turner, T., and Wendel, K., "The Influence of Stress on Aluminum Conductor Life", IEEE/IRPS, (1985), pp. 142-147.

15. Hosoda, T., Yagi, H., and Tsuchikawa, H., "Effects of Copper and Titanium Addition to Aluminum Interconnects on Electro- and Stress-Migration Open Circuit Failures", IEEE/IRPS, (1989), pp. 202-206.

16. Nix W.D., Course notes on "The Mechanical Properties of Thin Films", Course 207B, Stanford University, (1988).

17. Hertzberg, R.W., Deformation and Fracture Mechanics of Engineering Materials, John Wiley and Sons, (1976), p. 151.

18. Yost, F.G., Romig, A.D. Jr., and Bourcier, R.J., "Stress Driven Diffusive Voiding of Aluminum Conductor Lines: A Model for Time Dependent Failure", Sandia Report, Sand88-0946, Distribution Category UC-25, (August 1988), p. 17.

19. Bird, J.E., Mukherjee, A.K., and Dorn, J.E., Quantitative Relations Between Properties and Microstructure, Israel University Press, Haifa, Israel, (1969), p. 255.

20. Hertzberg, R.W., Deformation and Fracture Mechanics of Engineering Materials, John Wiley and Sons, (1976), p. 154.

21. Mott N.F., and Narabbo F.R.N., "Report on Strength of Solids", Physical Society, (1948), P. 1.

22. McLellan, R.B., and Ishikawa, T., "The Elastic Properties of Al at High Temperatures", J. Phys. Chem. Solid, Vol. 48, (1987), P. 603.

23. Pizzo P.P., "Rate Equations for Elevated Temperature

Creep", Transactions of the ASME, Vol. 101, (Oct. 1979), P. 396.

24. Barrett C.R., Nix W.D., and Tetelman A.S., Principles of Engineering Materials, Prentice-Hall, Inc., (1973), P. 279.

25. Ashby, M.F., and Brown L.M., Perspectives in Creep Fracture, Pergamon, (1983), p. 26.

26. Ashby, M.F., "A First Report on Deformation-Mechanism Maps", Acta Metallurgica, Vol. 20, (July 1972), pp. 887-897.

27. Black J., "RADC-TR-77-410 Final Technical Report", (Dec. 1977).

28. Attardo M.J., and Rosenberg R., "Electromigration Damage in Al Film Conductors", Journal of Applied Physics, Vol. 41, No. 6, (May 1970), P. 2381.